Open Location Management in Automated Warehousing Systems

Yugang YU and René B.M. de Koster

ERIM Report Series *Research in Management*	
ERIM Report Series reference number	ERS-2009-004-LIS
Publication	January 2009
Number of pages	43
Persistent paper URL	http://hdl.handle.net/1765/14615
Email address corresponding author	yyugang@rsm.nl
Address	Erasmus Research Institute of Management (ERIM) RSM Erasmus University / Erasmus School of Economics Erasmus Universiteit Rotterdam P.O.Box 1738 3000 DR Rotterdam, The Netherlands Phone: + 31 10 408 1182 Fax: + 31 10 408 9640 Email: info@erim.eur.nl Internet: www.erim.eur.nl

Bibliographic data and classifications of all the ERIM reports are also available on the ERIM website:
www.erim.eur.nl

ERASMUS RESEARCH INSTITUTE OF MANAGEMENT

REPORT SERIES
RESEARCH IN MANAGEMENT

ABSTRACT AND KEYWORDS	
Abstract	A warehouse needs to have sufficient open locations to be able to store incoming shipments of various sizes. In combination with ongoing load retrievals open locations gradually spread over the storage area. Unfavorable positions of open locations negatively impact the average load retrieval times. This paper presents a new method to manage these open locations such that the average system travel time for processing a block of storage and retrieval jobs in an automated warehousing system is minimized. We introduce the effective storage area (ESA), a well-defined part of the locations closest to the depot; where only a part of the open locations –the effective open locations-, together with all the products, are stored. We determine the optimal number of effective open locations and the ESA boundary minimizing the average travel time. Using the ESA policy, the travel time of a pair of storage and retrieval jobs can be reduced by more than 10% on average. Its performance depends hardly on the number or the sequence of retrievals. In fact, in case of only one retrieval, applying the policy leads already to beneficial results. Application is also easy; the ESA size can be changed dynamically during storage and retrieval operations.
Free Keywords	distribution science, warehousing, AS/RS, storage and retrieval, open locations
Availability	The ERIM Report Series is distributed through the following platforms: Academic Repository at Erasmus University (DEAR), DEAR ERIM Series Portal Social Science Research Network (SSRN), SSRN ERIM Series Webpage Research Papers in Economics (REPEC), REPEC ERIM Series Webpage
Classifications	The electronic versions of the papers in the ERIM report Series contain bibliographic metadata by the following classification systems: Library of Congress Classification, (LCC) LCC Webpage Journal of Economic Literature, (JEL), JEL Webpage ACM Computing Classification System CCS Webpage Inspec Classification scheme (ICS), ICS Webpage

Open Location Management in Automated Warehousing Systems

Yugang YU
Rotterdam School of Management, Erasmus University, the Netherlands, yyugang@rsm.nl

René B.M. de Koster
Rotterdam School of Management, Erasmus University, the Netherlands, rkoster@rsm.nl

Draft version: Jan 2009

A warehouse needs to have sufficient open locations to be able to store incoming shipments of various sizes. In combination with ongoing load retrievals open locations gradually spread over the storage area. Unfavorable positions of open locations negatively impact the average load retrieval times. This paper presents a new method to manage these open locations such that the average system travel time for processing a block of storage and retrieval jobs in an automated warehousing system is minimized. We introduce the effective storage area (ESA), a well-defined part of the locations closest to the depot; where only a part of the open locations –the *effective* open locations-, together with all the products, are stored. We determine the optimal number of effective open locations and the ESA boundary minimizing the average travel time. Using the ESA policy, the travel time of a pair of storage and retrieval jobs can be reduced by more than 10% on average. Its performance depends hardly on the number or the sequence of retrievals. In fact, in case of only one retrieval, applying the policy leads already to beneficial results. Application is also easy; the ESA size can be changed dynamically during storage and retrieval operations.

Keywords: Distribution science, warehousing; AS/RS; storage and retrieval; open locations

---

1. Introduction

Warehouses are key nodes in supply chains. They decouple demand from supply in space, quantity, and time. They therefore play a crucial role in realizing high supply chain efficiency and service levels. Since the seminal papers of Hausmann et al. (1976), Graves et al. (1977), and Han et al., (1987), warehouse design and management have received vast attention in management literature.

In order to run a warehouse storage system efficiently, a sufficient number of open locations (or empty slots) are necessary. This number depends on the change of the inventory levels over time and the way the system operates. If the number is insufficient, much time can be required in storage (and later in retrieval) because of lack of chance to find an open location close to the depot for incoming storage loads or difficulty in pairing open locations and retrieval locations. According to Tompkins et al. (2003, p. 403), the rule of thumb in practice is: “when a warehouse is more than 80% full, more space is needed” and “this rule is based on the fact that when a warehouse reaches this capacity, it takes longer to put something away”. For automated unit load warehousing systems (where pallets or totes are stored and retrieved by a storage and retrieval -S/R- machine) several researchers (e.g., Graves et al., 1977; Han et al., 1987; Meller & Mungwattana, 1997) have shown that, for sequencing a given block of storage and retrieval jobs, the average travel time of an S/R-machine for a pair of storage and retrieval jobs decreases with an increasing number of available open locations (see Figure 1). The more open locations the system has, the easier the system finds them to store incoming loads, and to combine the storages with retrievals. However if the number of open locations increases beyond a bound, (e.g. m_e in Figure 1), increasing the number has little effect on further reducing the cycle travel time. However, although present in several results (reviewed in Section 2), this effect has not been noted in past literature.

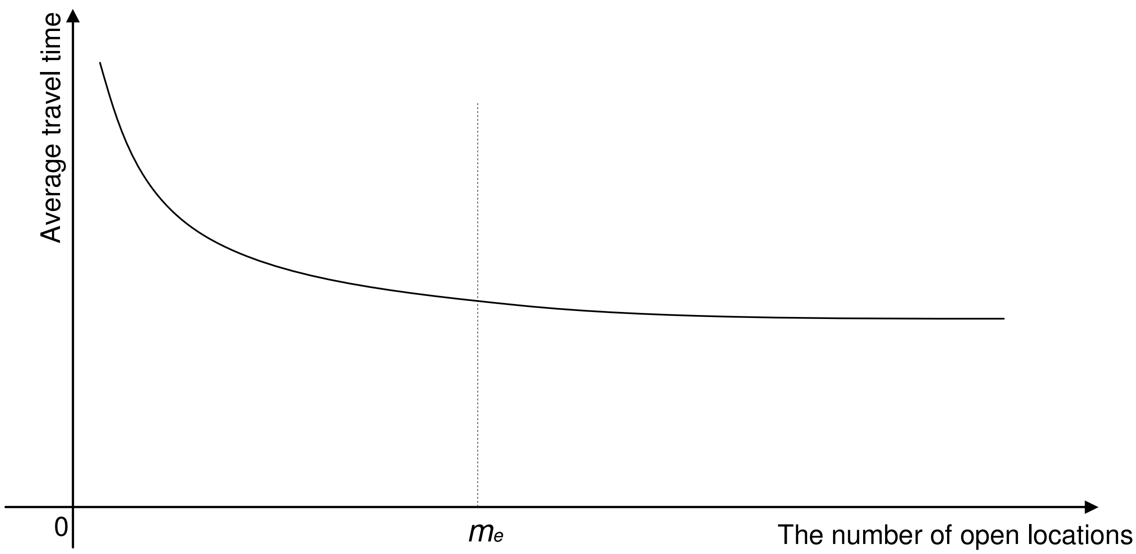

Figure 1: The Effect of the Number of Open Locations on the Average Travel Time of a Pair of Storage/Retrieval Jobs

We make use of this phenomenon by no longer allowing all the open locations (see Figure 2(a)) to be available to incoming storage jobs, but only those locations in an Effective Storage Area (ESA) (see Figure 2(b)). The ESA contains only a part of the open locations closest to the depot and all the products stored. The open locations within the ESA are called *effective* open locations. The other, or *ineffective* open locations, are located outside the ESA and form an Ineffective Storage Area (ISA) (see Figure 2(b)). In order to create an ESA of a given size, unit loads stored outside have to be swapped with inside open locations. Once the ESA has been created, it is easy to maintain. In situations where only double plays are carried out (a storage job combined with a retrieval) we only store and retrieve unit loads within the ESA. As stored products may have to be retrieved at any location within the entire ESA, after some time of operation, the open locations will be scattered randomly within the ESA and the ESA will look like in Figure 2(b).

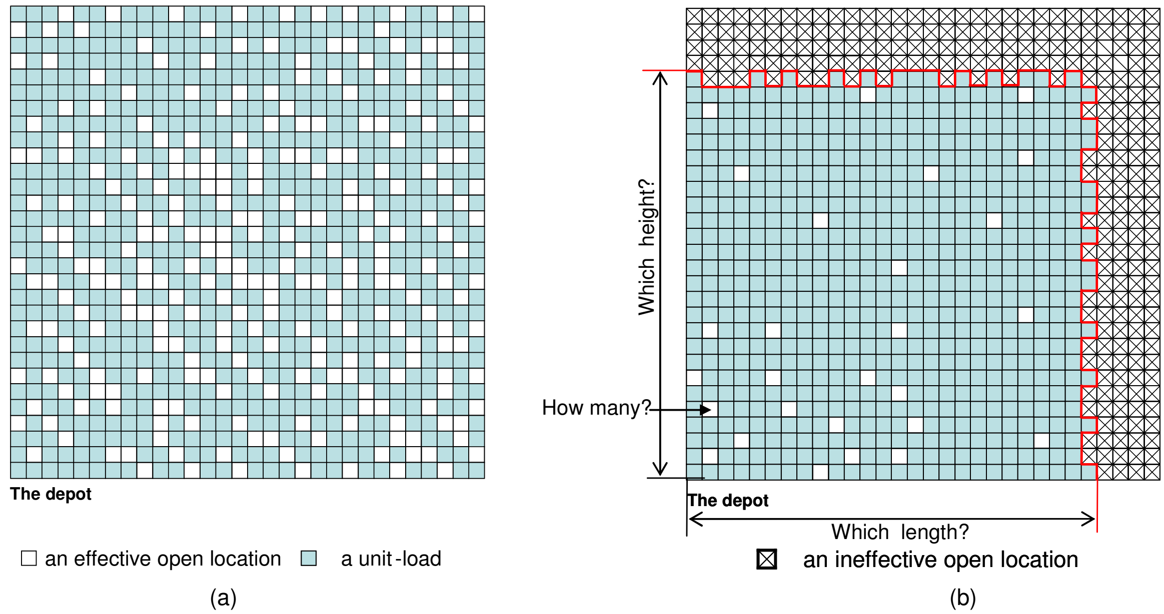

Figure 2: Effective Storage Area (ESA) and Ineffective Storage Area (ISA)

The number of effective open location influences the average storage and retrieval time as it determines, together with the given number of stored unit loads, the size of ESA. If the ESA contains too many open locations it becomes large, which negatively impacts the average storage and retrieval time. If it contains too few open locations, it is difficult to match a retrieval to a storage job closely leading to too long average storage and retrieval times. Our main research questions therefore are: (1) how many effective open locations (m_e) should the ESA have and (2) what is the optimal boundary of the ESA to minimize the average travel time of a pair of S/R jobs. Equivalently, we want to minimize the makespan of a given block of S/R jobs that have to be carried out.

Storing and retrieving loads using a shrunk and optimized ESA is intriguingly simple and intuitive. However, it has not been studied in previous literature. Although in practice many different storage policies are used, depending on situation and possibilities (like class-based storage, or pre-shuffling known future retrievals in idle periods), we are not aware of companies that persistently manage the positions of open locations. We show use of the ESA policy can lead to substantial reductions in average travel time for storage and retrieval jobs in case of random demand compared to the situation where open locations are not explicitly managed, i.e. they are scattered over the storage area.

We model the research problem for a given block of storage and retrieval jobs that have to be processed. The problem is complex due to the nonlinearity of the objective function, nonlinearity of constraints and integrality of the decision variable: the number of effective open locations, as we will show later. Fortunately, we can obtain the optimal solution numerically in an efficient way.

In the model we use the same warehousing system as described in several seminal papers (e.g. Hausman et al., 1976; Graves et al., 1977; Han et al., 1987), namely an automated storage and retrieval system (**AS/RS**). These systems have been widely used to replace conventional manual warehouses since the 1950s (Lee & Schaefer, 1996). Typically, an AS/RS consists of a storage/retrieval (**S/R**) machine, a storage rack, a depot (or I/O point), and products stored on unit-loads (standardized pallets or totes). The unit-loads enter and leave the system at the depot. They are stored and retrieved by the S/R machine to and from the storage rack. In an AS/RS, the S/R machine's capacity normally is one unit-load. Therefore the system can operate in two command modes:

Single-command Cycle (SC) mode: In a travel cycle of the S/R machine a single job, either a storage or a retrieval, is performed. To store a unit-load, the S/R machine picks up a unit-load from the depot, moves, and deliveries it to an open location. After that, the S/R machine returns to the depot to complete the SC. To retrieve a unit-load, the process is reversed.

Dual-command Cycle (DC) mode: In a travel cycle of the S/R machine a storage is paired with a retrieval. The S/R machine picks up a unit load from the depot to store it at an open location, and then moves emptily to a retrieval location to retrieve a unit-load. After this, the S/R machine returns to the depot and completes the DC. The empty travel time between the storage and retrieval location is called the *interleaving* travel time.

In operation, the DC mode is preferred because it can bring approximately 30% travel time reduction compared with the SC mode (Graves et al., 1977) for a pair of S/R jobs. Rather than comparing the performance of a single pair of storage and retrieval jobs, our research is based on processing a given block of dual command cycles (or S/R jobs). For this, a policy to sequence these DCs to has to be selected.

For a given block of S/R jobs, the unit loads to be stored arrive and commonly wait on an accumulating conveyor in front of the depot. Only the first load can be picked up by the S/R machine. Therefore storage jobs can only be served in a first-come first-served (*FCFS*) sequence. The storage locations can be selected among all open locations in the rack. Retrievals can be sequenced freely as every retrieval location in the rack face is reachable by the S/R machine. Therefore the sequencing policies mainly focus on how to pair an open location and a retrieval as a DC and how to sequence multiple retrievals. This paper adopts the nearest neighbor policy, which sequences retrieval jobs based on the interleaving distance between storage and retrieval locations. The smallest one is processed next.

The remainder of the paper is organized as follows. In Section 2, we review literature. In Section 3, we formulate a mathematical model to determine the optimal number of effective open locations and the boundary of the ESA. In section 4, we develop an algorithm to obtain the optimal solution of the model based on some solution properties. In section 5, we evaluate the ESA policy by various numerical examples. In Section 6, we discuss how to implement the ESA policy in practice. Lastly, in Section 7, we conclude the paper and provide some future research directions.

2. Literature Review

This section reviews papers related to open location selection, retrieval sequencing policies and the decreasing marginal effect of adding open locations illustrated in Figure 1.

Open location selection. To our knowledge, no academic literature directly focuses on open location management in terms of positioning and numbering of open locations. However there is some literature about open location selection where each time one open location is selected from all open locations for a storage job. For example, the COL (closest open locations) policy, as a storage policy, stores every incoming pallet at the open location closest to the depot (Schwarz et al. 1978). The implementation of the policy can form a forward area (closer to the depot) with pallets and few open locations, and a backward area (further from the depot) with open locations. However, due to lack of a proper management of the open locations, Schwarz et al. (1978) and some others have shown that eventually the COL performs almost at the same level as a pure random storage policy with a FCFS policy for storages and retrievals. All sequencing policies mentioned in the next two paragraphs also contain some rules about selecting open locations for storages. However, none consider explicitly managing open locations.

Retrieval sequencing. Optimal sequencing a block of storage and retrieval jobs is a NP hard problem under random or class-based storage (Han et al., 1987; Bozer & White, 1990; Gu et al., 2007). Therefore most literature focuses on solving the problem with various sequencing heuristic policies and storage policies such as FCFS (first-come-first-served) (Graves et al., 1977; Han et al., 1987; Gu et al., 2007), NN (nearest-neighbor) (Han et al., 1987), SDC (shortest dual command cycle) (Lee & Schaefer, 1996), and $1+\varepsilon$ optimization where ε indicates a tolerance gap between the objective value of a solution and a problem lower bound (Lee & Schaefer, 1996). In the above papers, the most frequently cited and effective policy to sequence a block of storage and retrieval jobs one is NN. Compared with FCFS for sequencing storages and retrievals and COL for storage locations, the results in the above papers show NN can increase the throughput by 10-15%, by reducing the *travel-between* time with 50% or more. The travel time savings depend on the number of open locations and the block size: the number of storage and retrieval jobs. The savings decrease for increasing numbers of open locations and increasing block size. Mahajan et al. (1998) have shown numerically that NN provides near optimal solutions with only 3-6% gaps from a lower bound. In experiments of Lee and Schaefer (1996) gaps are mostly within 4% from the optimal solution. Therefore NN has been adopted as retrieval sequencing heuristic by many researchers for different system configurations and demand patterns. Meller and Mungwattana (1997) for example, use NN and a variant (RNN-reverse nearest neighbor) for a multi-shuttle AS/RS where the S/R machine has twin- and triple-shuttles with quadruple-command or sextuple-command operational modes, respectively. Eben-Chaime (1992) uses NN as a dispatching rule in an AS/RS with stochastic demand and finds similar results. This paper therefore selects NN.

Decreasing marginal effect of increasing the number of open locations (Figure 1). This phenomenon, appears to exist in unit-load warehousing systems with different sequencing heuristics (e.g. Graves et al., 1977; Han et al., 1987; Lee & Schaefer, 1996), storage policies ((e.g. Graves et al., 1977; Lee & Schaefer, 1997), different types of retrieval machines (e.g. Meller & Mungwattana, 1997), and demand patterns (e.g. Schwarz et al., 1978; Eben-Chaime, 1992). As an example, Graves et al. (1977) study retrieval sequencing for an AS/RS with class-based storage. An inbound load has to be stored in its appropriate class. Then the first K jobs in the retrieval queue are sequentially examined to find a retrieval in the same class as the storage load to construct a DC. If no such load can be found the first job in the retrieval queue is selected. Schwarz et al.(1978) apply the same sequencing policy, under a dynamic setting. The block size changes dynamically due to stochastic product demand. Lee and Schaefer (1996) propose a shortest dual command cycle (SDC) heuristic and an ε -optimum algorithm for the sequencing problem, where ε indicates a tolerance gap between the objective value of a solution and a problem lower bound. They compare these heuristics and several other ones, such as *NN,* and shortest leg, for different system shapes and block sizes. Lee and Schaefer (1997) discuss a sequencing problem in an AS/RS using dedicated storage. Six algorithms, including a static assignment algorithm (ASSTA), a static heuristic algorithm (HRSTA), and a dynamic assignment algorithm (ASDYN), are tested. More examples for supporting the curve in Figure 1 can be found in (Sarker et al., 1991; Eynan & Rosenblatt, 1993; Van den Berg & Gademann, 1999), and some relevant review papers (Van den Berg, 1999; De Koster et al., 2007; Gu et al., 2007).. However, to our knowledge, disadvantages of the too many open locations are not studied yet.

3. Model Formulation

3.1 Assumptions and Notations

The assumptions for the system described in the introduction are as follows (see also Graves et al., 1977; Han et al., 1987):

- Storage and retrieval jobs are carried out one block after another. The system handles a new block of storage and retrieval jobs only when its preceding blocks have been completed. This assumption is relaxed in Section 6.
- The system operates in dual command cycle mode.

- The system objective is to minimize the expected travel time per DC.
- The total storage capacity, the speed of the depth movement mechanisms, and the S/R machine's speeds in the horizontal and vertical directions are known and constant.
- The depot is located at the lower left-hand corner of the rack.
- The rack is considered to be a continuous rectangular pick face.
- The machine can move simultaneously in horizontal and vertical directions, so that travel time is the maximum of horizontal travel time and vertical travel time. When the S/R machine is idle, it stops at the depot. The pick-up and deposit time of a load is not considered (this time is fairly constant for real systems).
- Storage jobs are performed in a FCFS sequence.
- The effective open locations for storage jobs and the retrieval locations for retrieval jobs are selected by the *NN* policy to form pairs of DCs.

The length (*L*) and the height (*H*) of the storage rack form the horizontal and vertical dimensions of the system. The speeds of the S/R machine in the horizontal and vertical directions are s_c and s_h, respectively. We define $t_h = L / s_h$ as length (in time) of the rack and $t_v = H / s_v$ as height (in time) of the rack. Let $T = \max\{t_h, t_v\}$ and $b = \min\{t_h, t_v\} / T$ represent the shape factor of the rack. If $b = 1$, we call the rack shape square-in-time (**SIT**), and **NSIT** (non-SIT) otherwise. Without loss of generality, we discuss the problem in the dimensions of $t_h \times t_v = 1 \times b$ by setting *T*=1. The corresponding results can then be generalized to other rectangular rack dimensions by multiplying them by $T \neq 1$ (see also Hausman et al., 1976; Han et al., 1987).

The other key notations are:

Sets and parameters:

C_N	The system storage capacity expressed in number of unit loads.
S and R	The sets of initial effective open and retrieval locations, respectively.

n The number of retrievals $|R|$, or the block size, or the number of DCs.

u Storage space utilization of the system.

m The total number of open locations in the rack, $m = C_N(1-u)$.

b_e The shape factor of the ESA, $b_e = y_e / x_e$.

ETB Expected travel-between (i.e., interleaving) time in a DC.

ESC Expected SC travel time.

EDC Expected DC travel time of a DC using the ESA policy.

EDC^{NN} Expected DC travel time of a DC without using the ESA policy (the NN policy is used).

Decision variables:

x_e The length (in time) of the ESA, $0 < x_e \le 1$.

y_e The height (in time) of the ESA, $0 < y_e \le \min(b, x_e)$. Without loss of generality, we assume $y_e \le x_e$.

m_e The number of effective open locations in the ESA, $m_e = |S|$.

3.2 Model

We obtain a model, denoted as M, to optimally dimension the ESA and determine m_e as follows:

Model M:

$$\min\ EDC(x_e, y_e, m_e) = ESC(x_e, y_e, m_e) + ETB(x_e, y_e, m_e) \tag{1}$$

$$\frac{(m_e + C_N \cdot u)}{C_N}(b \times 1) = x_e \cdot y_e \tag{2}$$

$$0 < x_e \le 1 \tag{3}$$

$$0 < y_e \le \min(b, x_e) \tag{4}$$

$$1 \le m_e \le m \tag{5}$$

Decision variables are x_e, y_e, m_e, and m_e is an integer.

The objective (1) is to minimize the expected *DC* travel time for the case where a block of *n* DCs is processed by the NN policy. The objective (1) is derived in Appendix A; $ESC(x_e, y_e, m_e)$ is calculated by:

$$ESC(x_e, y_e, m_e) = y_e^2 /(3x_e) + x_e \,, \tag{6}$$

and $ETB(x_e, y_e, m_e)$ is calculated by

$$ETB(x_e, y_e, m_e) = \frac{x_e}{n} \sum_{k=m_e}^{n+m_e-1} \int_0^1 z\, k[1 - F_e(z)]^{k-1} f_e(z) dz \,, \tag{7}$$

where

$$F_e(z) = \begin{cases} (2z - z^2)(\frac{z}{b_e})[2 - (\frac{z}{b_e})] & 0 < z \le b_e \\ 2z - z^2 & b_e < z \le 1 \end{cases} , \tag{8}$$

and $$f_e(z) = \begin{cases} 2(1-z)(\frac{z}{b_e})[2 - (\frac{z}{b_e})] + z(2-z)(\frac{2}{b_e})(1 - \frac{z}{b_e}) & 0 < z \le b_e \\ 2(1-z) & b_e < z \le 1 \end{cases} . \tag{9}$$

are the cumulative density function (CDF) and the probability density function (PDF), respectively. $b_e = x_e / y_e$ is the shape factor of the ESA.

Constraint (2) represents the ESA stores the all unit-loads ($C_N \cdot u$) and effective open locations (m_e). Constraints (3), (4) and (5) determine the lower and upper bounds for variables x_e y_e, and m_e, respectively.

Both the objective function (1) and constraint (2) are nonlinear. m_e is an integer variable. The model therefore is non-linear integer. With standard software such as Mathematica5.2 (2005), $ETB(x_e, y_e, m_e)$ cannot be evaluated analytically within a reasonable time (e.g. less than one hour) for realistic sizes of the rack and retrieval blocks. We therefore have to rely on numerical methods.

4. Algorithm and Properties

Because x_e and y_e are continuous variables, it is impossible to enumerate every combination to obtain an optimal solution of Model M. To simplify the computation process, in subsection 4.1 an algorithm is developed to obtain the optimal solution of Model M based on some properties. After that, Section 4.2 proves some other properties (Theorems 3-6) helpful in explaining numerical results.

4.1 Algorithm

The best ratio of x_e and y_e in the solutions of Model M is proved in Lemma 1 below. This lemma makes use of Lemma 2 (refer to Appendix B).

LEMMA 1. *Consider a given system with fixed* n, m *and* m_e, *and two different shapes of the ESA with the same area size. The shape of the ESA closer to SIT leads to a smaller value of* $EDC(x_e, y_e, m_e)$.

Proof. See Appendix C.

Based on Lemma 1, we obtain Theorem 1 to determine the optimal x_e^* and y_e^* as a function of m_e.

THEOREM 1. *For a given rack of dimensions 1×b, and a given* m_e *between 1 and m,*

(a) *if* $1 \le m_e \le C_N(b-u)$, *the shape of the optimal ESA is SIT and the optimal ESA dimensions as a function of* m_e *are*

$$x_e^*(m_e) = y_e^*(m_e) = \sqrt{(m_e + C_N \cdot u)b / C_N} \,. \tag{10}$$

(b) *if* $\max\{C_N(b-u),1\} < m_e \le m$, *the shape of the optimal ESA is NSIT and the optimal ESA dimensions are*

$$x_e^*(m_e) = (m_e + C_N \cdot u) / C_N \,, \tag{11}$$

$$y_e^*(m_e) = b \,. \tag{12}$$

Proof. According to Lemma 1, if the ESA can be feasibly constructed in SIT shape, it will be the optimum, otherwise the feasible non-SIT shape closest to the SIT (with the largest $b_e = y_e^*(m_e) / x_e^*(m_e)$)

will be the optimum. That is, for a given m_e the optimal $x_e^*(m_e)$ and $y_e^*(m_e)$ can be determined by the feasible ESA shape closest to the SIT.

For Theorem 1(a), because $m_e \le C_N(b-u)$ (i.e., $(m_e + C_N \cdot u)b / C_N \le b \cdot b$), we can construct a SIT shape (b_e=1) with $x_e^*(m_e) = y_e^*(m_e) = \sqrt{(m_e + C_N \cdot u)b / C_N}$, which does not violate any Constraints (1)-(5). Therefore, Equation (10) holds and Theorem 1(a) has been proved.

For Theorem 1(b), because $\max\{C_N(b-u),1\} < m_e \le m$ (i.e., $(m_e + C_N \cdot u)b / C_N > b \cdot b$), the shape of the ESA closest to SIT with feasible y_e makes Constraint (4) binding with $y_e^*(m_e)$ =*b*, while $x_e^*(m_e) = ((m_e + C_N \cdot u)b / C_N)$/*b*=$(m_e + C_N \cdot u) / C_N$. This results in the largest value of b_e. Therefore, Equations (11) and (12) hold and Theorem 1(b) has been proved.

Using Equations (10)-(12), we can simplify Model M by eliminating x_e or y_e. Model M can therefore be split into two sub-models; one is for the case: $1 \le m_e \le C_N(b-u)$ (denoted by Model M1) where the ESA is SIT, and the other is for the case: $\max\{C_N(b-u),1\} \le m_e \le m$ (denoted by Model M2) where the ESA is NSIT. We treat these models subsequently.

For Model M1 (only applicable if $C_N(b-u) \ge 1$), substituting Equation (10) into Equation (6), we obtain ESC as a function of m_e equaling

$$ESC(m_e) = 4\sqrt{(m_e + C_N \cdot u)b / C_N} / 3, \quad 1 \le m_e \le C_N(b-u). \qquad (13)$$

By substituting Equations (10) into Equation (7), we can obtain ETB as a function of m_e equaling

$$ETB(m_e) = \frac{1}{n} \sum_{k=m_e}^{n+m_e-1} [\sqrt{(m_e + C_N \cdot u)b / C_N} \int_0^1 zk[1 - F_e(z)]^{k-1} f_e(z) dz], .1 \le m_e \le C_N(b-u). \; (14)$$

The objective function of Model M1 is now a function of m_e, denoted as $EDC(m_e)$, and is the sum of Equations (13) and (14).

For the constraints of Model M1, we replace Constraints (2)-(4) of Model M with $1 \le m_e \le C_N(b-u)$.

For Model M2, in analogy to Model M1, ESC, as a function of m_e, equals

$$ESC(m_e) = b^2 / (3(m_e + C_N \cdot u) / C_N) + (m_e + C_N \cdot u) / C_N, \tag{15}$$

and ETB equals

$$ETB(m_e) = \frac{1}{n} \sum_{k=m_e}^{n+m_e-1} [(m_e + C_N \cdot u) / C_N \int_0^1 zk[1 - F_e(z)]^{k-1} f_e(z) dz], \tag{16}$$

where $\max\{C_N(b-u), 1\} \le m_e \le m$.

The objective function for Model M2 is the sum of Equations (15) and (16).

The constraints of Model M2 are obtained by replacing Constraints (2)-(4) with $\max\{C_N(b-u), 1\} \le m_e \le m$.

Therefore, the overall optimal solution is the optimal solution of either Model M1 or Model M2 that provides the minimum objective value. As Model M1 and Model M2 both are a function of a single decision variable m_e, they then can be solved optimally by enumerating m_e between 1 and *m* considering their constraints on m_e.

Theorem 2 below shows it is not necessary to enumerate every m_e for finding the optimal m_e^*.

THEOREM 2. *$EDC(m_e)$ has a unique global minimum in Models M where $EDC(m_e)$ is the combination of objective functions of Models M1 and M2 given in Equations* (13)-(16).

Proof. See Appendix D.

Normally $EDC(m_e)$ is not a convex function of m_e although it is a “U” (or partly “U”) -shape function. According to Theorem 2, we can choose golden section search (Press et al., 2007) to find m_e^* and then use Theorem 1 to determine (x_e^*, y_e^*) by the following algorithm steps:

Step 0 (*system initialization*): Set the system capacity C_N, the system utilization u, the shape factor *b*, and the number of retrievals *n*.

Step 1 (*set initial values of m_e for the golden section search*): Set lower and upper bounds for the number `of m_e; The lower bound (denoted as *LB*) is set to be 1, and the upper bound (denoted as *UB*) is

$\lceil C_N \cdot (1-u) \rceil$. We set a starting point m_e =min ($\lfloor C_N \cdot (1-u) \rfloor$, $\lfloor C_N \cdot 3\% \rfloor$) for m_e^*. The closer the starting point m_e is to the optimum m_e^*, the shorter the computation time of the algorithm.

Step 2 (*recall the golden section search*): During the computation, for every given m_e, $EDC(m_e)$ can be calculated by Model M1 if $1 \le m_e \le C_N(b-u)$ or M2 if $\max\{C_N(b-u),1\} \le m_e \le m$. During the computation, *UB* and *LB* are updated using a golden section search (Press et al., 2007) to narrow down [*LB*, *UB*] with $LB \le m_e^* \le UB$. As m_e is integer, *LB* and *UB* are rounded up and down respectively to be integer at every update. As UB and LB are integers, the convergence condition to obtain m_e^* can be set as:

$$UB - LB = 0 \tag{17}$$

Step 3 (*output the optimal solutions*): If the condition (17) is satisfied, output m_e^*, and $EDC^*(x_e^*, y_e^*, m_e^*)$. After this, according to Theorem 1, x_e^*, y_e^* can be obtained by using m_e^*.

4.2 Some Other Properties

The phenomenon described in Figure 1 can be proved by Theorem 3, and a similar phenomenon for EDC as a function of *n* can be proved by Theorem 4. In these two theorems, the ESA policy is not used (by setting $m_e = m$, x_e =1 and y_e =*b* in Model M).

THEOREM 3. *For a fixed n, with an increase in m,*

(a) EDC^{NN} *decreases,*

(b) *the marginal reduction in* EDC^{NN} *decreases.*

Proof. See Appendix E.

THEOREM 4. *For a fixed m, with an increase in n,*

(a) EDC^{NN} *decreases,*

(b) *The marginal reduction in* EDC^{NN} *decreases.*

The proof of Theorem 4 is similar to Theorem 3, and is omitted here.

Theorem 5 below shows that an increase in m has more effect on reducing EDC^{NN} than the same increase in n does.

THEOREM 5. *Based on a given m and n, an increase in m brings a larger reduction of* EDC^{NN} *than the same amount of increase in n does.*

Proof. See Appendix F.

Although Theorem 5 is implicit in the numerical results of some literature, like Han et al. (1987), it has not been explicitly noted before. It can be understood by noticing that an added open location (*m)* can provide one more candidate storage location for all the DCs in the block of DCs, to reduce its travel time. However, an added retrieval can only reduce its own DC travel time while it may increase the total travel time of its previous DCs.

If the ESA policy is used ($m_e \le m$), we can derive a theorem similar to Theorem 4:

THEOREM 6. *The minimal expected DC travel time,* $EDC^*(x_e^*, y_e^*, m_e^*)$ *, is a decreasing function of n.*

Proof. See Appendix G.

However, $EDC^*(x_e^*, y_e^*, m_e^*)$ generally is not a convex function of n because, with an increase in n, m_e^* and the optimal ESA shape factor $b_e^* = y_e^* / x_e^*$ change simultaneously.

5. Numerical Examples

This section conducts numerical experiments to evaluate how much the ESA policy can outperform NN under various combinations of different parameters: the rack shape b, the system capacity C_N, the system utilization u, and the number of retrievals n.

5.1 Experimental Setup

We start with a base example with the parameter values: u=0.75, $b = 0.75$, C_N=1500, and n=20. After that we vary C_N, b, u, and n in the ranges of [500, 3000], [0.25, 1], [0.55, 0.95], and [1, 100], respectively. These values are based on expert judgments, and cover parameter values used in previous papers (e.g., Han et al., 1987; Lee & Schaefer, 1996). Moreover, we have tested examples with all possible combinations of C_N =500, 1000, 1500, 2000, 2500, 3000, b =0.25, 0.5, 0.75, 1, u =0.55, 0.65, 0.75, 0.85, 0.95, and n =1, 5, 10, 20, 30, 50, 100.

The algorithm steps are programmed in C++, and run on a DELL D630 notebook with CPU Duo 2.4 GHz, and 2GB of RAM. All results are normalized to a rack area of 1 square seconds by setting $T = (1/\sqrt{b})$.

5.2 Results

For the base example, the results are (x_e^*, y_e^*, m_e^*) = (0.90, 0.87, 43), and EDC^* =1.23 when using the ESA policy. Using NN yields an expected DC travel time of EDC^{NN} =1.39. Hence, EDC^* outperforms EDC^{NN} by 11.5%. Obviously, the phenomenon described by Figure 1 (proved by Theorem 3 for the NN policy) does not hold if the ESA policy is used.

The results corresponding to the sensitivity analyses of C_N , b , u , and n are shown in Figures 3-6 respectively. In each figure, the optimal number of open locations m_e^* , EDC^* , and EDC^{NN} are provided. The computation time of each instance evaluated is within a second.

From Figures 3-6 and the other related results, we obtain the following observations.

1) Figures 3-6 show the ESA policy reduces the DC travel time significantly. For all the possible combinations we have tested, the ESA policy outperforms NN by 14.5% on average.
2) The optimal number of effective open locations, m_e^* , depends on n , C_N , b , and u . m_e^* decreases with an increase in n while it increases with an increase in C_N , and b .

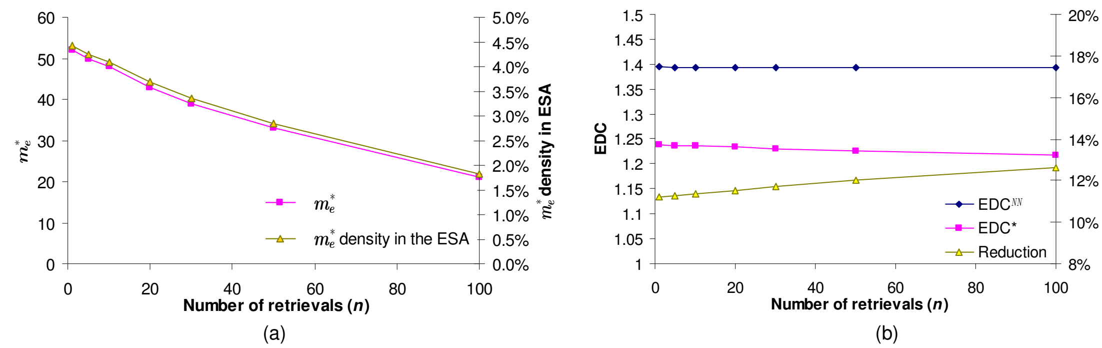

Note. m_e^* density in the ESA = (m_e^*/(the capacity of the ESA in number of unit loads))×100%.

Figure 3: Influence of the Number of Retrievals (i.e. Block Size n) on m_e^* and *EDC*

3) Open locations have more impact in reducing the average travel time than the same number of retrievals; In Figure 3, the values of EDC^* at (n=1, m=52) and (n=100, m=21) are almost the same, which means that the contribution of 100-1=99 retrievals in reducing *EDC* can be approximately replaced by 52-21=31 open locations if the ESA policy is applied. To some extent, this can be explained by Theorem 5.

4) EDC^* is quite insensitive to the number of retrievals n (i.e., the block size of DCs) although Theorem 6 holds. Figure 3(b) shows EDC^* decreases by less than 1% if n changes from 1 to 100. Executing retrievals one by one (i.e. n=1) is only slightly worse than cleverly sequencing them in a block size as large as 100. A similar phenomenon happens to EDC^{NN} in spite of Theorem 4. However, in many past papers (e.g., Han et al., 1987), it is stated that an increase in number of retrievals or a good sequence of retrievals can bring a significant reduction in the DC travel time. The "contradiction" can be explained by using Theorem 7 (see Appendix H); which states that the for large m there is a much smaller marginal effect of increasing n than for smaller values of m. In those previous papers fewer open locations tested (mostly less than 15) than the number (m_e) in the ESA policy (between 21 and 52 in Figure 3(a)). In practice, m normally is more than 50 even for a system with a high space utilization of 90% and low capacity of 500 unit loads. In conclusion, the larger number of open locations in our cases makes increasing retrievals have little impact on reducing *EDC*.

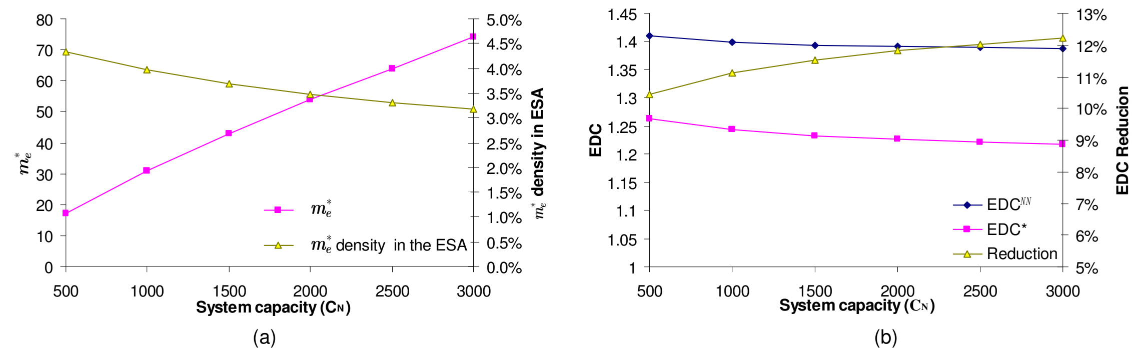

Note. m_e^* density in the ESA = (m_e^*/(the capacity of the ESA in number of unit loads))×100%.

Figure 4: Influence of System Capacity (C_N) on m_e^* and *EDC*

5) With an increase in the system capacity (C_N), the DC travel time reduction of the ESA policy over NN increases. In Figure 4(b), it can be seen that the reduction increases from 10.5% at C_N=500 to 12.2% at C_N=3000. The reason can be found in Figure 4(a); with increasing C_N, the density of m_e^* in the ESA decreases from 4.3% at C_N=500 to 3.2% at C_N=3000. This leads to a relatively smaller size of the ESA, and contributes to the increase of the reduction.

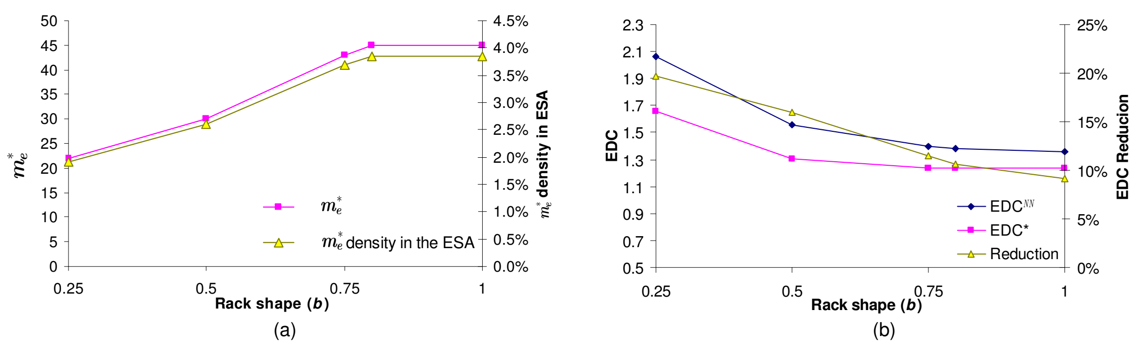

Note. m_e^* density in the ESA = (m_e^*/(the capacity of the ESA in number of unit loads))×100%.

Figure 5: Influence of Rack Shape (b) on m_e^* and *EDC*

6) Figure 5 shows the performance of the ESA policy is less sensitive to a change of the rack shape factor b compared with that of NN. Moreover, the skewer (smaller b) the rack shape is, the larger improvement the ESA policy obtains over NN (see Figure 5(b)).

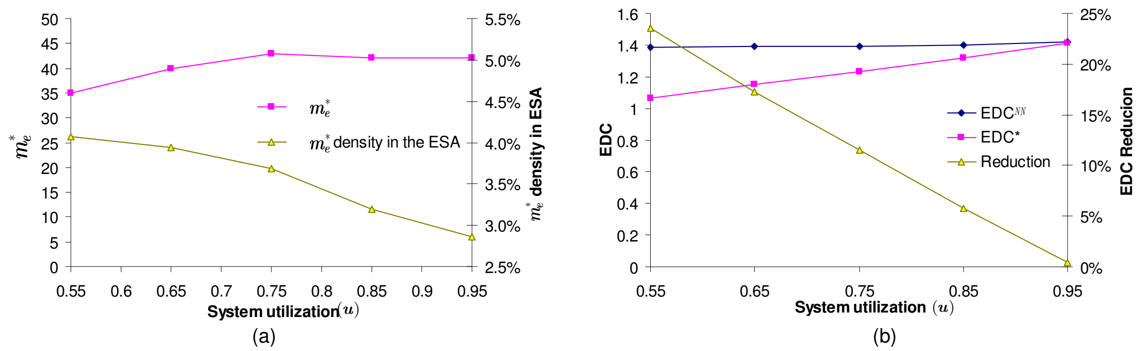

Note. m_e^* density in the ESA = (m_e^* /(the capacity of the ESA in number of unit loads))×100%.

Figure 6: Influence of System Utilization (u) on m_e^* and EDC

7) Figure 6 shows the reduction of the DC travel time of EDC^* over EDC^{NN} highly depends on the system utilization (u). If the system utilization u=0.55, the reduction reaches 23.5%. However, when u=0.95, the reduction is less than 1%. For common values of u between 0.65 and 0.85, the reductions are between 6% and 17%, which become larger if b becomes smaller.

8) m_e^* is not very sensitive to changes in u. Figure 6(a) shows increasing u from 0.75 to 0.95 does not cause an increment of m_e^* at all. This is due to the combined effect of the decrease in y_e^* / x_e^* (the shape of the ESA) and the increase of the ESA size. From observation 4 we know decreasing y_e^* / x_e^* reduces m_e^*. On the other hand, increasing the size of the ESA increases m_e^*. The two combined effects obviously outweigh each other for a great deal.

6. Implementing the ESA Policy in Practice

Figure 3(b) shows *EDC** is rather insensitive to the size of *n: EDC** at *n*=1 hardly differs from *EDC** at *n*=50. This leads to a valuable suggestion for implementing the ESA policy in practice:

Fix the block size n=1, and the number of effective open locations, m_e *to be* m_e^* *(at given n=1).*

With this we can obtain a near-optimal solution of the ESA policy, while the implementation becomes much easier as the number of effective open locations in the ESA is fixed regardless of the block size. We can even handle retrievals in block sizes of 1, for example by retrieving them in sequence of urgency, without noticeable impact on the expected DC travel time.

The suggestion is very easy to implement as n=1. Still, according to Theorem 4, a larger block size can reduce the DC travel time further. We can simply dynamically change n, in line with the queue length of waiting storage and retrieval jobs. We therefore suggest the following implementation.

Keep the block size ,n, equal to the queue length of storage and retrieval jobs, and fix the number of effective open locations (m_e) to be m_e^* for n=1.

For the base example in Section 5, the first suggestion obtains a near optimal *EDC* solution with maximum gaps of 0.97% from the optimum for n=50, where the "gap" is the gap between *EDC** at n=50 and *EDC** at n=1. The gap becomes 0.2% by using the second suggestion.

We have tested the above suggestions for a wide variety of possible combinations of C_N, b, u, and n (see Section 5.1) with similar results.

These suggestions show the first assumption in Subsection 3.1 can be relaxed. We do not have to fix the block size beforehand, but we can dynamically adapt it with close to optimal results.

In line with past research (e.g., Graves et al., 1977; Han et al., 1987), we so far have only considered DC modes. In this mode, once the ESA has been created, it can be maintained automatically. However, in practice we may be forced to carry out single-command cycles sometimes. The system utilization and then (m_e^*, x_e^*, y_e^*) may have to be changed correspondingly. In case of storage jobs only, m_e drops below m_e^*, and in case of only retrieval jobs m_e *exceeds* m_e^*. To see what the impact is of this is, we deliberately let m_e deviate from m_e^* within a given range between m_e^* at n=1 (i.e., m_e^*=52), and m_e^* at n=30 (i.e., m_e^*=39). Figure 7(a) shows *EDC* increases by less than 0.2% for the base example. We then test all the combinations of C_N, b, u, and n (given in Section 5.1). The results show that *EDC* deviates from *EDC** by less than 1% for $C_N \geq 1000$, and for most cases of C_N=500. Therefore, we can dynamically change (m_e, x_e, y_e), while *EDC* deviates little from *EDC**. This small deviation of *EDC* from *EDC** can be explained by looking at Figure 7(b). The difference becomes large only when m_e is quite far from m_e^*.

If the number of effective open locations deviates too far from the optimum, the optimal situation can be restored in idle periods.

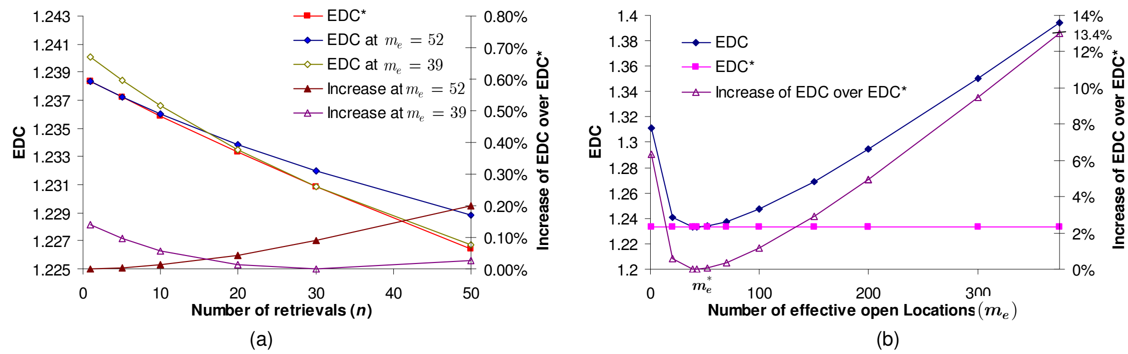

Note. m_e=52 and 39 correspond to the optimal m_e at n=1 and 30, respectively; *EDC* represents the result by substituting a fixed *m* and the results of Theorem 1 into Equation (1); "Increase at m_e=39" represents the increase of *EDC* at m_e=39 over EDC^*.

Figure 7: Influence of the Number of Effective Open Locations (m_e) on *EDC*

In conclusion, the implementation of the ESA policy is quite easy and flexible. With a change of *n* and *u*, the number of effective open locations (m_e), and the boundary, $x_e \times y_e$, of the ESA can be well managed without extra effort.

7. Conclusions and Further Research

To our knowledge, this paper is the first to focus on modeling the management of open locations in warehouses. We propose the ESA policy to manage open locations for minimizing the cycle travel time of a block of storage and retrieval jobs. A model, some properties and an algorithm are developed to determine the optimal number of open locations, and the boundary of the ESA. From the results of the paper, we obtain the following managerial insights:

- The ESA policy can outperform nearest neighbor (NN) by between 17% and 6% of the cycle travel time for realistic rack utilizations between 65 and 85%. Savings can be more than 20% if the system utilization is less than 65%.
- The optimal solution of the model depends on system capacity, system shape, and rack utilization. Our algorithm can determine the optimal number of open locations and the ESA boundary within a second for any real practical system size on an ordinary computer.

- Application of the ESA policy is fairly easy by using the suggestions in section 6. The suggestions make it possible to apply the ESA policy in varying conditions, even when the job queue changes or when there are only single commands to be performed.

We obtain several findings differing from those in previous research.

- The block size, *n*, of storage and retrieval jobs normally has little influence on the average DC travel time. However, all previous papers (e.g., Han et al., 1987; Lee & Schaefer, 1996; Mahajan et al., 1998) demonstrate that a large block size can significantly reduce the DC travel time. This can be explained as in these papers, due to calculation complexity, the number of open locations has only been evaluated for small values, e.g. <10. In practice the number of open locations in such a system is usually much larger. A typical aisle in an AS/RS system of about 70 pallets long and 10 pallets high contains 1400 pallets; with 95% rack utilization this implies 70 empty slots. The optimal number of effective open locations is normally less than 40 in such case.
- Changing the sequence of retrieval jobs normally has little influence on the DC travel time. As sufficient effective open locations are readily available in practice, our research, supported by Theorems 5&6 and numerical examples, shows that NN reduces the DC travel time mainly due to the smart selection of open locations, rather than cleverly sequencing retrievals.

The above differences greatly reinforce the advantages of the ESA policy. According to our first suggestion in Section 6 it is not necessary to intentionally lengthen the queue of retrievals in practice, especially as accumulating retrievals needs waiting time. The policy can be used dynamically by considering new incoming jobs and job urgency with little impact on the travel time.

This paper may trigger a new sub-research area in warehousing and distribution science to study the management of open locations. Based on this paper, further research directions at least include:

- Open location management in different warehousing systems: AS/RSs with multiple shuttles, end-of-aisle AS/RS systems, carousel systems, and conventional multi-aisle systems.

- Open location management under different storage policies: class-based storage, dedicated storage, duration-of-Stay (DOS), etc.
- Combinations of open location management with S/R machine dwell point selection, product prepositioning, etc.
- The possible effects of open location management on different warehousing system designs, such as system dimensions, and depot selection problems.
- Finally, with the increasing application of compact 3D storage warehouses (Yu & De Koster, 2008), open locations can also be managed for reducing the total cycle travel time in such systems. However, because open locations normally change dynamically during storage and retrieval processes in these systems, the related research could be much more challenging than in a conventional warehousing system.

References

Bozer, Y. A., & White, J. A. (1984). Travel-time models for automated storage/retrieval systems. *IIE Transactions*, 16, 329-338.

Bozer, Y. A., & White, J. A. (1990). Design and performance models for end-of-aisle order picking systems. *Management Science*, 36(7), 852-866.

De Koster, R., Le-Duc, T., & Roodbergen, K. J. (2007). Design and control of warehouse order picking: A literature review. *European Journal of Operational Research*, 182(2), 481-501.

Dooly, D. R., & Lee, H. F. (2008). A shift-based sequencing method for twin-shuttle automated storage and retrieval systems. *IIE Transactions*, 40(6), 586-594.

Eben-Chaime, M. (1992). Operations Sequencing in Automated Warehousing Systems. *International Journal of Production Research*, 30(10), 2401-2409.

Eynan, A., & Rosenblatt, M. J. (1993). An Interleaving Policy in Automated Storage-Retrieval Systems. *International Journal of Production Research*, 31(1), 1-18.

Graves, S. C., Hausman, W. H., & Schwarz, L. B. (1977). Storage-retrieval interleaving in automatic warehousing systems. *Management Science*, 23, 935-945.

Gu, J. X., Goetschalckx, M., & McGinnis, L. F. (2007). Research on warehouse operation: A comprehensive review. *European Journal of Operational Research*, 177(1), 1-21.

Han, M. H., McGinnis, L. F., Shieh, J. S., & White, J. A. (1987). On sequencing retrievals in an automated storage/retrieval system. *IIE Transactions*, 19(1), 56-66.

Hausman, W. H., Schwarz, L. B., & Graves, S. C. (1976). Optimal storage assignment in automatic warehousing systems. *Management Science*, 22(6), 629-638.

Lee, H. F., & Schaefer, S. K. (1996). Retrieval sequencing for unit-load automated storage and retrieval systems with multiple openings. *International Journal of Production Research*, 34(10), 2943-2962.

Lee, H. F., & Schaefer, S. K. (1997). Sequencing methods for automated storage and retrieval systems with dedicated storage. *Computers & Industrial Engineering*, 32(2), 351-362.

Mahajan, S., Rao, B. V., & Peters, B. A. (1998). A retrieval sequencing heuristic for miniload end-of-aisle automated storage/retrieval systems. *International Journal of Production Research*, 36(6), 1715-1731.

Mathematica5.2 (2005). Wolfram Research, Inc.

Meller, R. D., & Mungwattana, A. (1997). Multi-shuttle automated storage/retrieval systems. *IIE Transactions*, 29(10), 925-938.

Press, W. H., Teukolsky, S. A., Vetterling, W. T., & Flannery, B. P. (2007). *Numerical Recipes: The Art of Scientific Computing (3 ed.)*. Cambridge: Cambridge University Press.

Sarker, B. R., Sabapathy, A., Lal, A. M., & Han, M. H. (1991). Performance evaluation of a double shuttle automated storage and retrieval system. *Production Planning & Control*, 2(3), 207-213.

Schwarz, L. B., Graves, S. C., & Hausman, W. H. (1978). Scheduling policies for automatic warehousing systems: simulation results. *IIE Transactions*, 10(3), 260-270.

Tompkins, J. A., White, J. A., Bozer, Y. A., & Tanchoco, J. M. A. (2003). *Facilities Planning*. New York: John Wiley and Sons.

Van den Berg, J. P. (1999). A literature survey on planning and control of warehousing systems. *IIE Transactions*, 31(8), 751-762.

Van den Berg, J. P., & Gademann, A. J. R. M. (1999). Optimal routing in an automated storage/retrieval system with dedicated storage. *IIE Transactions*, 31(5), 407-415.

Yu, Y., & De Koster, M. B. M. (2008). Optimal zone boundaries for two-class-based compact three-dimensional automated storage and retrieval systems. *IIE Transactions*, 41(3), 194-208.

Appendices:

Appendix A. Estimation and Validation of *EDC*

For a given block size, n, of storage and retrieval jobs, NN processes the jobs by the following procedure (Han et al., 1987):

While $R \neq \varnothing$,

1. Select a pair (s, r), $s \in S$ and $r \in R$, with minimum travel-between time.
2. Perform the DC, by storing s and retrieving r.
3. $R \leftarrow R - \{r\}$.
4. $S \leftarrow S - \{s\} + \{r\}$.

End.

The average travel time of a DC, *EDC*, equals the average single command travel time, *ESC*, plus the average travel-between time of n DCs, ETB.

According to Han et al. (1987) and Mahajan et al. (1998), using NN, *ESC* can be estimated by:

$$ESC = b^2 / 3 + 1, \tag{18}$$

for a 1×b storage rack. This basic formula was derived by Bozer and White (1984) and is based on a FCFS sequence for storages and retrievals and purely random selection of open locations.

If the rack face is split into an ESA and an ISA, and the boundary of the ESA is $x_e \times y_e$ ($x_e \geq y_e$), we have Equation (6).

For ETB, Bozer and White (1984) show that the distance Z between two randomly selected locations in a 1×b storage rack is a random variable with a cumulative density function (CDF) and a probability density function (PDF):

$$F(z) = P(Z \leq z) = \begin{cases} (2z - z^2)(\frac{z}{b})[2 - (\frac{z}{b})] & 0 < z \leq b \\ 2z - z^2 & b < z \leq 1 \end{cases},$$

and $$f(z)=\begin{cases}2(1-z)(\frac{z}{b})[2-(\frac{z}{b})]+z(2-z)(\frac{2}{b})(1-\frac{z}{b}) & 0<z\le b\\ 2(1-z) & b<z\le 1\end{cases}.$$

Given a sample of k random distances, Han et al. (1987) show that the smallest of them, $Z_k^{\min}$, $0<Z_k^{\min}\le 1$, is a random variable with the PDF:

$$g_k(Z_k^{\min})=k[1-F(Z_k^{\min})]^{k-1}f(Z_k^{\min})\quad 0<Z_k^{\min}\le 1. \tag{19}$$

Therefore, the expected value of the smallest travel-between time, $E(Z_k^{\min})$, on a $1\times b$ rack equals

$$E(Z_k^{\min})=\int_0^1 z\,g_k(z)dz=\int_0^1 z\,k[1-F(z)]^{k-1}f(z)dz. \tag{20}$$

In Han et al. (1987), the total expected travel-between time for n DCs is estimated by $\sum_{k=m_e}^{n+m_e-1}E(Z_k^{\min})$, and ETB is then estimated by:

$$ETB=\frac{1}{n}\sum_{k=m}^{n+m-1}E(Z_k^{\min})\quad 0<Z_k^{\min}\le 1. \tag{21}$$

If the ESA policy is applied, the distance Z between two randomly selected locations in an $x_e\times y_e$ ESA is a random variable. If Z normalized to a $1\times b_e$ ESA, its CDF and PDF are in Equations (8) and (9) respectively. The smallest of k random distances, $Z_k^{\min}(x_e,y_e,m_e)$ on the $1\times b_e$ ESA has the PDF:

$$\bar{g}_k(Z_k^{\min})=k[1-F_e(Z_k^{\min})]^{k-1}f_e(Z_k^{\min})\quad 0<Z_k^{\min}\le 1. \tag{22}$$

$E(Z_k^{\min}(x_e,y_e,m_e))$ on an $x_e\times y_e$ ESA becomes:

$$E(Z_k^{\min}(x_e,y_e,m_e))=x_e\int_0^1 z\,\bar{g}_k(z)dz=x_e\int_0^1 z\,k[1-F_e(z)]^{k-1}f_e(z)dz. \tag{23}$$

In analogy to the derivation of Equation (21), $ETB(x_e,y_e,m_e)$ can be estimated by

$\sum_{k=m_e}^{n+m_e-1}E(Z_k^{\min}(x_e,y_e,m_e))/n$ which gives Equation (7).

Therefore, we obtain Equation (1) using Equations (6) and (7).

The estimates in Equations (18) and (21) (a special case of Equations (6) and (7) with m_e=m) have been validated by previous researchers including Han et al. (1987) and Dooly and Lee (2008). They show the estimate is quite accurate. Therefore Equation (1) with m_e=m (or Equation (18) plus (21)) has been used in many papers (e.g., Eynan & Rosenblatt, 1993; Meller & Mungwattana, 1997). We repeat the validation of Equation (1) for wide ranges of $1 \le n \le 100$ and $1 \le m_e \le 2000$ by using Monte Carlo simulation. With a confidence level of 95% and a confidence interval as the average DC value× (1±1.5%), the simulations (with 83160 replications) show that the analytic estimates are all within the given confidence interval. The estimates are therefore accurate and are used in this paper.

Appendix B. Lemma 2 and Its Proof

LEMMA 2. *Let* $B(k) = \int_0^1 u(z)\,\overline{g}_k(z)dz$ *where* $u(z)$ *is a function of z,* 0≤*z*≤1, *k is a positive integer and* $\overline{g}_k(z)$ *is defined by Equation* (22)*. We have*

(a) $\overline{g}_{k+1}(z) \ge \overline{g}_k(z)$ *for* $0 \le z \le F_e^{-1}(1/(k+1))$, *and* $\overline{g}_{k+1}(z) \le \overline{g}_k(z)$ *for* $F_e^{-1}(1/(k+1)) \le z \le 1$.

(b) $B(k) \ge B(k+1)$ *if* $u(z)$ *is an increasing function of z where "=" only holds for* $u(z)$ *being a constant*.

(c) $B(k) \le B(k+1)$ *if* $u(z)$ *is a decreasing function of z where "=" only holds for* $u(z)$ *being a constant*
(d) $B(k) = 0$ *if* $u(z)$ =0.
Proof. For (a), by changing *k* to *k*+1, we have

$$\overline{g}_{k+1}(z) - \overline{g}_k(z) = (k+1)(1-F_e(z))^k f_e(z) - k(1-F_e(z))^{k-1} f_e(z)$$

$$= [(k+1)(1-F_e(z)) - k]\cdot(1-F_e(z))^{k-1} f_e(z). \tag{24}$$

Letting $\overline{g}_{k+1}(z) - \overline{g}_k(z)$ =0, we have $z = F_e^{-1}(1/(k+1))$ where 0< $F_e^{-1}(1/(k+1))$ <1 as 0<1/(*k*+1)<1.

In Equation (24), because $f_e(z)(1-F_e(z))^{k-1}$ >0, and (1- $F_e(z)$) is a decreasing function of *z*, we have

$$\overline{g}_{k+1}(z) - \overline{g}_k(z) \begin{cases} \ge 0 & \text{if} \quad 0 \le z \le a \\ < 0 & \text{if} \quad a < z \le 1 \end{cases}.$$

where $a = F_e^{-1}(1/(k+1))$. Therefore (a) has been proved.

For (b), $B(k+1) - B(k) = \int_0^1 u(z)\,\overline{g}_{k+1}(z)dz - \int_0^1 u(z)\,\overline{g}_k(z)dz = \int_0^1 u(z)[\overline{g}_{k+1}(z) - \overline{g}_k(z)]dz$.

$= \iint_{R_1} u(z)dydz - \iint_{R_2} u(z)dydz$ where $R_1 = \{(y,z) \mid 0 \le z \le a, \overline{g}_k(z) \le y \le \overline{g}_{k+1}(z)\}$, $R_2 = \{(y,z) \mid a \le z \le 1,$

$\overline{g}_{k+1}(z) \le y \le \overline{g}_k(z)\}$.

Because $u(z)$ is an increasing function of *z*, we have

$$\iint_{R_1} u(z)dydz \le \iint_{R_1} u(a)dydz \text{ , and } \iint_{R_2} u(a)dydz \le \iint_{R_2} u(z)dydz \ . \tag{25}$$

Where "=" only holds for $u(z)$ being a constant.

Because $\overline{g}_k(z)$ (i.e., Equation (19)) is a PDF,

$$\int_0^1 \overline{g}_k(z)\,dz = \int_0^1 k[1-F_e(z)]^{k-1} f_e(z)\,dz = 1,\ \forall k \text{ is a positive integer,} \tag{26}$$

we have $\iint_{R_1} dydz = \iint_{R_2} dydz$. As $u(a)$ is a constant, we have

$$\iint_{R_1} u(a)dzdy = \iint_{R_2} u(a)dzdy \ . \tag{27}$$

Using Equations (25) and (27), we have $\iint_{R_1} u(z)dzdy \le \iint_{R_2} u(z)dzdy$. That is $B(k+1)-B(k) \le 0$ ("=" only holds for $u(z)$ being a constant) and (b) has been proved.

In analogy to the Proof of (b), (c) and (d) can be easily proved and their proofs are omitted here.

Appendix C. Proof of LEMMA 1

To keep the ESA equally sized, while changing its shape, without loss of generality we normalize the ESA area to have size=1 by setting $x_e = 1/\sqrt{b_e}$ and $y_e = \sqrt{b_e}$.

According to Bozer and White (1984), for a storage area $(1/\sqrt{b_e}) \times \sqrt{b_e}$,

$$ESC(x_e, y_e, m_e) = \frac{2}{\sqrt{b_e}}\left(\int_0^{b_e} \frac{2z^2}{b_e}dz + \int_{b_e}^1 zdz\right).$$

Next, from Equations (7)-(9), for a storage area $(1/\sqrt{b_e}) \times \sqrt{b_e}$ we have

$$E(Z_k^{\min}(x_e, y_e, m_e)) = x_e\int_0^{b_e} P_A dz + x_e\int_{b_e}^1 P_B\, dz \ . \tag{28}$$

where $P_A = \frac{2kz^2(4b_e - 3(1+b_e)z + 2z^2)((b_e^2 + 2b_e(-2+z)z^2 + (2-z)z^2)/b_e^2)^k}{b_e^2 - 4b_e z^2 + 2(1+b_e)z^3 - z^4}$, and $P_B = 2k(1-z)^{2k-1}z$.

$$ETB(x_e, y_e, m_e) = (\frac{1}{n}\sum_{k=m_e}^{n+m_e-1}\int_0^{b_e} P_A dz + \frac{1}{n}\sum_{k=m_e}^{n+m_e-1}\int_0^{b_e} P_B dz)/\sqrt{b_e}.$$

$EDC(x_e, y_e, m_e) = ESC(x_e, y_e, m_e) + ETB(x_e, y_e, m_e)$ can now be expressed as a function of b_e (denoted as $EDC(b_e)$). We have $EDC(b_e) = \int_0^{b_e}(\frac{4z^2}{b_e\sqrt{b_e}} + \frac{1}{n}\sum_{k=m_e}^{n+m_e-1}\frac{P_A}{\sqrt{b_e}})dz + \int_{b_e}^1(\frac{2z}{\sqrt{b_e}} + \frac{1}{n}\sum_{k=m_e}^{n+m_e-1}\frac{P_B}{\sqrt{b_e}})dz$.

We can prove Lemma 1 by demonstrating that $EDC(b_e)$ is a decreasing function of b_e (i.e., $dEDC(b_e)/db_e \le 0$ with $0 < b_e \le 1$).

$$\frac{dEDC(b_e)}{db_e} = f_1(b_e, b_e) - f_2(b_e, b_e) + \int_0^{b_e}\frac{\partial}{\partial b_e}(\frac{4z^2}{b_e\sqrt{b_e}} + \frac{1}{n}\sum_{k=m_e}^{n+m_e-1}\frac{P_A}{\sqrt{b_e}})dz + \int_{b_e}^1\frac{\partial}{\partial b_e}(\frac{2z}{\sqrt{b_e}} + \frac{1}{n}\sum_{k=m_e}^{n+m_e-1}\frac{P_B}{\sqrt{b_e}})dz$$

$$= f_1(b_e, b_e) - f_2(b_e, b_e) + \int_0^{b_e}\frac{\partial}{\partial b_e}(\frac{4z^2}{b_e\sqrt{b_e}})dz + \int_{b_e}^1\frac{\partial}{\partial b_e}(\frac{2z}{\sqrt{b_e}})dz + \int_0^{b_e}\frac{\partial}{\partial b_e}(\frac{1}{n}\sum_{k=m_e}^{n+m_e-1}\frac{P_A}{\sqrt{b_e}})dz + \int_{b_e}^1\frac{\partial}{\partial b_e}(\frac{1}{n}\sum_{k=m_e}^{n+m_e-1}\frac{P_B}{\sqrt{b_e}})dz,$$

where $f_1(b_e, z) = \frac{4z^2}{b_e\sqrt{b_e}} + \frac{1}{n}\sum_{k=m_e}^{n+m_e-1}\frac{P_A}{\sqrt{b_e}}$, and $f_2(b_e, z) = \frac{2z}{\sqrt{b_e}} + \frac{1}{n}\sum_{k=m_e}^{n+m_e-1}\frac{P_B}{\sqrt{b_e}}$.

Because $f_1(b_e, b_e) - f_2(b_e, b_e) = 2\sqrt{b_e}$, $\int_0^{b_e}\frac{\partial}{\partial b_e}(\frac{4z^2}{b_e\sqrt{b_e}})dz = -2\sqrt{b_e}$, and $\int_{b_e}^1\frac{\partial}{\partial b_e}(\frac{2z}{\sqrt{b_e}})dz = -b_e^{-3/2}(1-b_e) \le 0$

(where "=" only holds at $b_e=1$), we have $\frac{dEDC(b_e)}{db_e} \le V(b_e)$ where

$V(b_e) = \int_0^{b_e}\frac{\partial}{\partial b_e}(\frac{1}{n}\sum_{k=m_e}^{n+m_e-1}\frac{P_A}{\sqrt{b_e}})dz + \int_{b_e}^1\frac{\partial}{\partial b_e}(\frac{1}{n}\sum_{k=m_e}^{n+m_e-1}\frac{P_B}{\sqrt{b_e}})dz$, and "=" only holds at $b_e=1$.

$\frac{dEDC(b_e)}{db_e} \le 0$ therefore can be proved by demonstrating $V(b_e) \le 0$.

By rearranging the sequence of summation and differentiation we obtain

$$V(b_e) = \int_0^{b_e}(\frac{1}{n}\sum_{k=m_e}^{n+m_e-1}\frac{\partial}{\partial b_e}(\frac{P_A}{\sqrt{b_e}}))dz + \int_{b_e}^1(\frac{1}{n}\sum_{k=m_e}^{n+m_e-1}\frac{\partial}{\partial b_e}(\frac{P_B}{\sqrt{b_e}}))dz.$$

We analyze both right-hand side terms separately. For $\int_0^{b_e}(\frac{1}{n}\sum_{k=m_e}^{n+m_e-1}\frac{\partial}{\partial b_e}(\frac{P_A}{\sqrt{b_e}}))dz$, we have

$$\frac{d}{db_e}(\frac{P_A}{\sqrt{b_e}})=z\,k(k-1)[1-F_e(z)]^{k-2}(F_e(z))'_{b_e}f_e(z)b_e^{-1/2}+z\,k[1-F_e(z)]^{k-1}(f_e(z))'_{b_e}b_e^{-1/2}$$

$-0.5z\,k[1-F_e(z)]^{k-1}f_e(z)b_e^{-3/2}=\int_0^{b_e}\overline{g}_k(z)h_k(z)dz$ where $\overline{g}_k(z)$ refers to Equation (22) and

$$h_k(z)=\frac{z((1+4k)(z-2)z^4(2z-3)+3b_e^3(3z-4)-b_e(z-2)z^3(-14+9z+4k(5z-7))}{2b_e^{3/2}(4b_e-3(1+b_e)z+2z^2)(b_e^2+2b_e(z-2)z^2-(z-2)z^3)}$$

$$+\frac{b_e^2z^2(15+2z(2k(z-2)(3z-4)+(z-3)(3z-1)))}{2b_e^{3/2}(4b_e-3(1+b_e)z+2z^2)(b_e^2+2b_e(z-2)z^2-(z-2)z^3)}.$$

$\partial h_k(z)/\partial k$ can be proven to be smaller than 0. Therefore, we have

$$h_k(z)\le h_1(z),\quad k\ge 1 \text{ and integer}$$

where $h_1(z)=\frac{3b_e(4-3z)+5z(-3+2z)}{2b_e^{3/2}((3-2z)z+b_e(-4+3z))}$ for $0\le z\le b_e$.

Because $\overline{g}_k(z)$ is a PDF with $\overline{g}_k(z)\ge 0$ for $0\le z\le b_e$, according to Lemma 2(c), we have

$$\int_0^{b_e}\overline{g}_k(z)h_k(z)dz\le\int_0^{b_e}\overline{g}_k(z)h_1(z)dz. \tag{29}$$

For the second term, $\int_{b_e}^1(\frac{1}{n}\sum_{k=m_e}^{n+m_e-1}\frac{\partial}{\partial b_e}(\frac{P_B}{\sqrt{b_e}}))dz$, we have

$$\frac{\partial}{\partial b_e}(\frac{P_B}{\sqrt{b_e}})=-\frac{k(1-z)^{2k}z}{b_e^{-3/2}(1-z)}=\int_{b_e}^1\overline{g}_k(z)(-0.5zb_e^{-3/2})dz\le\int_{b_e}^1\overline{g}_k(z)\cdot 0dz=\int_{b_e}^1\overline{g}_k(z)h_1(z)dz \tag{30}$$

where $h_1(z)$=0, $b_e\le z\le 1$. We can then set

$$h_1(z)=\begin{cases}\frac{3b_e(4-3z)+5z(-3+2z)}{2b_e^{3/2}((3-2z)z+b_e(-4+3z))} & 0\le z\le b_e\\ 0 & b_e\le z\le 1\end{cases} \tag{31}$$

Using Equations (29) and (30), we have

$$V(b_e)\le\int_0^1[\frac{1}{n}\sum_{k=m_e}^{n+m_e-1}\overline{g}_k(z)h_1(z)]dz=\frac{1}{n}\sum_{k=m_e}^{n+m_e-1}[\int_0^1\overline{g}_k(z)h_1(z)dz] \tag{32}$$

According to Equation (32), we can prove $V(b_e) \le 0$ by demonstrating $\int_0^1 \overline{g}_k(z)h_1(z)dz \le 0$ ($k \ge 1$ and integer).

Let $H(k) = \int_0^1 \overline{g}_k(z)h_1(z)dz$ ($k \ge 1$ and integer). To prove $\int_0^1 \overline{g}_k(z)h_1(z)dz \le 0$, we distinguish two steps.

Step 1 is to prove

$$H(k) \le \max\{H(+\infty), H(1)\} \tag{33}$$

Step 2 is to prove

$$\max\{H(+\infty), H(1)\} \le 0. \tag{34}$$

Step 1. We distinguish six sub-steps. Step 1.1 proves $h_1(z)$ is a convex function of *z*, $z \in [0, b_e]$; Step 1.2 proves $h_1(z)$ reaches its minimum at a *z* (denoted as z_0) within $(0, b_e)$, and its maximum at *z*=0 or *b*; Step 1.3 shows that $h_k(z)$ can be split into decreasing, increasing and constant functions of *z* in three respective domains: [0, z_0], [z_0, b_e] and [b_e, 1]; Step 1.4 shows that one upper bound of $H(k)$ may be obtained at $H(+\infty)$; Step 1.5 shows one upper bound of $H(k)$ may be obtained at $H(1)$; Step 1.6 demonstrates that $\max\{H(+\infty), H(1)\}$ is an upper bound of $H(k)$.

Step 1.1. $\dfrac{d^2h_1(z)}{dz^2} = \dfrac{4(z^3 + 3b_e(z-2)(4+3(z-2)z))}{\sqrt{b_e}((3-2z)z + b_e(3z-4))^3}$. We can prove that $4(z^3 + 3b_e(z-2)(4+3(z-2)z))<0$ and $\sqrt{b_e}((3-2z)z + b_e(3z-4))^3<0$ for $0 < z < b_e$. Therefore $d^2h_1(z)/dz^2>0$, and Step 1.1 has been proved.

Step 1.2. $\dfrac{dh_1(z)}{dz} = \dfrac{-3b_e^2(4-3z)^2 - 5(3-2z)^2z^2 + 12b_e z(10+z(5z-14))}{2b_e^{3/2}((3-2z)z + b_e(3z-4))^2}$. Substituting *z*=0 into it, we have $\dfrac{dh_1(z)}{dz} = -1.5b_e^{3/2} < 0$. Similarly, substituting $z = b_e$ into it, we have $\dfrac{dh_1(z)}{dz} = \dfrac{27 + b_e(13b_e - 36)}{2(b_e-1)^2 b_e^{3/2}}$ >0.

Therefore, there must be a *z* (denoted as z_0) satisfying $\dfrac{dh_1(z)}{dz}$=0. As $h_1(z)$ is a convex function of *z*, $h_1(z)$ reaches its minimum at $z = z_0$, and maximum at *z*=0 or b_e. Step 1.2 has been proved.

Step 1.3. Combining the result obtained in Step 1.2 and the definition of $h_1(z)$ in Equation (31), $h_1(z)$ can be split into three parts:

Part 1: $h_1(z)$ is a decreasing function of z at $0 \le z \le z_0$;

Part 2: $h_1(z)$ is an increasing function of z at $z_0 \le z \le b_e$; and

Part 3: $h_1(z)$=0 is constant at $b_e \le z \le 1$.

Step 1.4. From Step 1.2 we know one local maximum value of $h_1(z)$ is obtained at z=0. According to Lemma 2 (a), we know all the density value $\overline{g}_k(z)$ can only focus on z=0^+ at k=+∞ with

$\lim_{k\to+\infty}\int_0^1 \overline{g}_k(z)h_1(z)dz = \int_0^1 \overline{g}_{k\to+\infty}(z)h_1(z)dz = h_1(0)$, which may therefore be an upper bound of $H(k)$.

Step 1.5. As k decreases, high density values (measured by $\overline{g}_k(z)$) of $h_1(z)$ move gradually at higher values of z (i.e. closer to 1). The last such a decrease of k is from k=2 to 1. According to the proof of Lemma 2(b), we can obtain $H(2) \le H(1)$ if

$$\iint_{R_1} h_1(z)dydz \le \iint_{R_2} h_1(z)dydz, \qquad (35)$$

where $R_1 = \{(y,z) \mid 0 \le z \le a, \overline{g}_2(z) \le y \le \overline{g}_1(z)\}$, $R_2 = \{(y,z) \mid a \le z \le 1 \ , \overline{g}_1(z) \le y \le \overline{g}_2(z)$. $a = F_e^{-1}(1/2)$ is the intersection point of $\overline{g}_2(z)$ and $\overline{g}_1(z)$.

In this case, $H(1)$ can be an upper bound of $H(k)$.

If Equation (35) does not hold, $H(1)$ will not be an upper bound of $H(k)$. However, we show later this has no impact on the result.

Step 1.6. To prove Equation (33), we can equivalently prove, if there is a local maximum of $H(k)$ at $k = k^*$ for any $k^* \in (1, +\infty)$, then $H(k^*) \le H(+\infty)$.

As $H(k)$ reaches a local maximum at k= k*, we then have

$$H(k^*+1) \le H(k^*) \ge H(k^*-1). \qquad (36)$$

According to Lemma 2(a), with the increase in k from k^*-1 to k^*, the density of $h_1(z)$ (i.e., weighted with $\bar{g}_k$) becomes higher at $z \le a = F_e^{-1}(1/k^*)$, while it becomes lower at $z \ge a$,

$H(k^*) \ge H(k^*-1)$ represents that, with *k* changing from *k*-1 to *k*, the value of $h_1(z)$ at $z \le a$ is relatively higher than at $z \ge a$.

For $h_1(z)$ at $z \le a$, according to Step 1.3, $h_1(z)$ is a decreasing function of *z* for $0 \le z \le z_0$. Moreover, according to Step 1.3, if $z_0 \le a$, $h_1(z)$ becomes a increasing function of *z* at $z_0 \le z \le a$. Therefore, for $z \le a$, $h_1(z)$ reach its maximum either at $h_1(0)$ or $h_1(a)$. Then

$H(k^*) = \int_0^1 \bar{g}_{k^*}(z) h_1(z) dz \le \int_0^1 \bar{g}_{k^*}(z) \max(h_1(0), h_1(a)) dz$.

According to Lemma 2(b), we have $h_1(0) \ge h_1(a)$ because $H(k^*) \ge H(k^*-1)$ holds. We have

$H(k^*) \le \int_0^1 \bar{g}_{k^*}(z) \max(h_1(0), h_1(a)) dz = \int_0^1 \bar{g}_{k^*}(z) h_1(0) dz$.

For $\int_0^1 \bar{g}_{k^*}(z) h_1(0) dz$, following the proof in Lemma 2(b), we have $\int_0^1 \bar{g}_{k^*}(z) h_1(0) dz = \int_0^1 \bar{g}_{k \to +\infty}(z) h_1(z) dz$

$= H(+\infty)$. That is to say, $H(k^*) = \int_0^1 \bar{g}_{k^*}(z) h_1(z) dz \le H(+\infty)$.

That is, $H(k) \le H(+\infty)$. Step 1.6 and then Step 1 have then been proved.

Step 2. $H(1) = \int_0^1 \bar{g}_1(z) h_1(z) dz = -(1-b_e)\sqrt{b_e}/4 \le 0$, and $H(+\infty) = \int_0^1 \bar{g}_{n=+\infty}(z) h_1(z) dz = h_1(0) = -3/(2b_e^{3/2}) < 0$.

We obtain Equation (34).

Therefore we have $V(b_e) \le 0$, and then $\frac{dEDC(b_e)}{db_e} < 0$ for $0 < b_e < 1$. Lemma 1 has been proved.

Appendix D. Proof of THEOREM 2

From Equations (13)-(16), the objective function (1), as a function of m_e, becomes

$$EDC(m_e) = ESC(m_e) + ETB(m_e).$$

We can prove Theorem 2 by demonstrating that $dEDC(m_e)/dm_e$ either is a monotonous function of m_e, or has a unique global minimum. Without loss of generality, we assume m_e is a continuous variable, $1 \le m_e \le m$ here. The theorem can be proved in three Steps. Step 1 calculates $dEDC(m_e)/dm_e$ and analyzes some properties of Model M1 for further analysis; Steps 2, 3 and 4 prove that Model M1, M2 and then M have the property in Theorem 2 respectively.

Step 1. For Model M1, the ESA is SIT, and we have

$$\frac{dESC(m_e)}{dm_e} = \frac{d(4x_e^*(m_e)/3)}{dx_e} \cdot \frac{d(\sqrt{(m_e + C_N \cdot u)b/C_N})}{dm_e} = \frac{2b}{3x_e^*(m_e)C_N},$$

For $ETB(m_e)$, we have $\frac{dETB(m_e)}{dm_e} = \frac{1}{n}\sum_{k=m_e}^{n+m_e-1}\int_0^1 \frac{d(x_e^*(m_e)zk[1-F_e(z)]^{k-1}f_e(z))}{dm_e}dz$

$$= \frac{1}{n}\sum_{k=m_e}^{n+m_e-1}\{\int_0^1 \frac{d(x_e^*(m_e))}{dm_e} \cdot zk[1-F_e(z)]^{k-1}f_e(z)dz + \int_0^1 x_e \frac{d(k)}{dm_e} z[1-F_e(z)]^{k-1}f_e(z)dz$$
$$+\int_0^1 x_e^*(m_e)k \cdot \frac{d(z[1-F_e(z)]^{k-1}f_e(z))}{dm_e}dz\}$$
$$= \frac{1}{n}\sum_{k=m_e}^{n+m_e-1}\{\int_0^1 \frac{d(x_e^*(m_e))}{dm_e} zk[1-F_e(z)]^{k-1}f_e(z)dz + \int_0^1 x_e^*(m_e)z[1-F_e(z)]^{k-1}f_e(z)dz$$

$+\int_0^1 x_e^*(m_e)zk[1-F_e(z)]^{k-1}f_e(z)\ln(1-F_e(z))dz\}$, where $\frac{dx_e^*(m_e)}{dm_e} = \frac{b}{2C_N\sqrt{b(m_e + C_N \cdot u)/C_N}}$ >0.

Therefore we have

$$\frac{dEDC(m_e)}{dm_e} = Part1 + Part2 + Part3,$$

where $Part1 = \frac{2b}{3x_e^*(m_e)C_N}$, $Part2 = \frac{1}{n}\sum_{k=m_e}^{n+m_e-1}\{\int_0^1 \frac{d(x_e^*(m_e))}{dm_e} zk[1-F_e(z)]^{k-1}f_e(z)dz + \int_0^1 x_e^*(m_e)z[1-F_e(z)]^{k-1}f_e(z)dz\}$,

and $Part3 = \frac{1}{n}\sum_{k=m_e}^{n+m_e-1}\int_0^1 x_e^*(m_e)zk[1-F_e(z)]^{k-1}f_e(z)\ln(1-F_e(z))dz$. Unfortunately, $dETB(m_e)/dm_e$ is not analytically integrable. We therefore analyze the properties of these three parts for the further proof.

$Part1 > 0$ as $b > 0, x_e > 0, C_N > 0$. Moreover, it converges to 0 *polynomially* with the increase in m_e as $2b/(3x_eC_N)$ is positive with x_e given by Equation (10).

$Part2 > 0$ as $f_e(z) \geq 0$, $1 - F_e(z) \geq 0$, $x_e^*(m_e)$>0 and $\dfrac{dx_e^*(m_e)}{dm_e} > 0$ where all the "=" can only hold at the extreme points of *z*=0 or 1. Moreover, it equals 0 if *z*=0. And if *z*<1 $Part2$ converges to 0 *exponentially* with the increase in m_e as m_e is on the power of $1 - F_e(z)$ and $0 \leq 1 - F_e(z) < 1$.

$Part3 < 0$ as $f_e(z) \geq 0$, $0 \leq 1 - F_e(z) \leq 1$, and $\ln(1 - F_e(z)) \leq 0$ where all the "=" can only hold at the extreme points of *z*=0 or 1. Moreover, Part3 equals 0 if *z*=0. And if *z*<1 $Part3$ converges to 0 *exponentially* with the increase in m_e as m_e is on the power of $1 - F_e(z)$ and $0 \leq 1 - F_e(z) < 1$.

Step 2. There are three possible cases for the result of $dEDC(m_e)/dm_e$; Case 2.1: $dEDC(m_e)/dm_e > 0$, Case 2.2: $dEDC(m_e)/dm_e$<0, and Case 2.3: Otherwise.

Case 2.1. In this case, $EDC(m_e)$ reaches its minimum at $m_e = 1$.

Case 2.2. if $dEDC(m_e)/dm_e < 0$ for m_e =1, 2,…,*m*, then $EDC(m_e)$ reaches its minimum at $m_e = m$.

Case 2.3. There is at least one m_e satisfying $dEDC(m_e)/dm_e = 0$. Denote the smallest m_e satisfying $dEDC(m_e)/dm_e = Part1 + Part2 + Part3$=0 as m_0. That is $Part1 + Part2 = |Part3|$ at m_0. From the above analysis, with the increase in m_e, $Part1 + Part2$ converges to 0 *polynomially* with the increase in m_e as $Part1$ converges to 0 polynomially and $Part2$ converges to 0 exponentially. Meanwhile, $Part3$=0 for *z*=0, or converges to 0 exponentially with the increase in m_e for *z*>0. It means that ,with increasing m_e ,once $Part1 + Part2 = |Part3|$ at m_0, $|Part3|$ will become less than $Part1 + Part2$ (converging to 0 polynomially) at $m_e > m_0$. That is, for $m > m_0$, $Part1 + Part2$ -$|Part3| = Part1 + Part2 + Part3$ $= dEDC(m_e)/dm_e$ will be positive, and converges to 0. Moreover, as $dEDC(m_e)/dm_e$>0 for $m_e > m_0$, and m_0 is the smallest to make $dEDC(m_e)/dm_e$=0 at $m_e = m_0$, we have $dEDC(m_e)/dm_e \leq 0$ for $m_e < m_0$.

Therefore we have, for Model M1, $EDC(m_e)$ has a unique global minimum. It is a decreasing function of m_e if m_e is less than m_0, and an increasing function of m_e if m_e is larger than m_0.

Step 3. For Model M2, using a similar process, we can prove the property for Model M2. Note that for the proof, $Part3$ will become more complex as b_e will not be 1, and is a function of m_e. However, it does not change the property that $Part3$=0 or converges to 0 exponentially with the increase in m_e.

Step 4. From the result of Steps 2&3, if $C_N(b-u) \le 1$ or $C_N(b-u) \ge m$, Model M1 or M2 is equivalent to Model M. The properties in Theorem 2 hold for Model M. Otherwise, $1 < C_N(b-u) < m$. In this case, $m_e = C_N(b-u)$ is the intersection point (denoted as m_i) of the objective functions of Model M1 & M2. At $m_e = m_i$, there are four possible cases for $dEDC(m_e)/dm_e$. Case 4.1: $dEDC(m_e)/dm_e \le 0$ for both Model M1&M2, Case 4.2: $dEDC(m_e)/dm_e \ge 0$ for both Model M1&M2, Case 4.3: $dEDC(m_e)/dm_e \ge 0$ for Model M1, but ≤ 0 for Model M2, and Case 4.4: $dEDC(m_e)/dm_e \le 0$ for Model M1, but ≥ 0 for Model M2.

Case 4.1. For Model M1, if $dEDC(m_e)/dm_e \le 0$ at $m_e = C_N(b-u)$, according to the proof in Step 2, we have $dEDC(m_e)/dm_e \le 0$ for all $m_e \le C_N(b-u)$. $EDC(m_e)$ obtains its minimum at $m_e = C_N(b-u)$.

For Model M2, because $dEDC(m_e)/dm_e \le 0$ at $m_e = C_N(b-u)$ and $EDC(m_e)$ is a continuous function of m_e for $m_e \in [1,m]$, the minimal value $EDC(m_e)$ of Model M1 is only a feasible solution of Model M2. With the result in Step 3, the unique global optimal value m_e of Model M2 will become the optimal value m_e^* of Model M.

Case 4.2. For Model M2, according to the proof in Step 2, $dEDC(m_e)/dm_e \ge 0$ for all $m_e \ge C_N(b-u)$, and $EDC(m_e)$ gets the minimum at $m_e = C_N(b-u)$. For Model M1, because $dEDC(m_e)/dm_e \ge 0$ at $m_e = C_N(b-u)$ and $EDC(m_e)$ is a continuous function of m_e for $m_e \in [1,m]$, the minimal value $EDC(m_e)$ of Model M2 is only a feasible solution of Model M1. With the result in Step 2, the unique global optimal value m_e of Model M1 will become the optimal value m_e^* of Model M.

Case 4.3. We prove that this case does not exist by reduction to absurdity. For Model M1, $dEDC(m_e)/dm_e \geq 0$ at $m_e = C_N(b-u)$. According to the proof in Case 2, if m_e increases further to an m_e while the ESA shape still keeps in SIT, $EDC(m_e)$ would increase to a high value (denoted as EDC'). Moreover, according to Lemma 1, this value is less than any other value of $EDC(m_e)$ in NSIT, which corresponds to a solution of Model M2. Denoting the NSIT value of Model M2 as EDC'', we obtain $EDC'' > EDC' > EDC(m_e)\big|_{m_e=C_N(b-u)}$, which contradicts $dEDC(m_e)/dm_e \leq 0$ for Model M2. We therefore can eliminate this case.

Case 4.4. For Model M1, if $dEDC(m_e)/dm_e \leq 0$ at $m_e = C_N(b-u)$, according to the proof in Step 2, we have $dEDC(m_e)/dm_e \leq 0$ for all $m_e \leq C_N(b-u)$. Similarly, for Model M2, $dEDC(m_e)/dm_e \geq 0$ for all $m_e \geq C_N(b-u)$. We therefore have $m_e = C_N(b-u)$ is the global optimal solution m_e^* of Model M.

Summarizing the cases 4.1-4.4, we obtain that $EDC(m_e)$ is a decreasing function of m_e if m_e is less than m_e^*, and an increasing function of m_e if m_e is larger than m_e^*. Therefore Step 4 is done and Theorem 2 has been proved.

Appendix E. Proof of THEOREM 3

Because the ESA dimensions and the rack dimensions are identical. *ESC* is not a function of m according to Equation (18) (or (6) with $m_e = m$, $x_e = 1$ and $y_e = b$). To prove Theorem 3, it suffices to prove that ETB in Equation (21) (or (7) with $m_e = m$, $x_e = 1$ and $y_e = b$) has the properties mentioned in Theorem 3.

For Theorem 3(a), we can prove it by showing $ETB\big|_{m=l+1} - ETB\big|_{m=l}$ <0, l=1, 2,…,C_N-1.

According to Equation (7), if m increases from l to $l+1$, we have

$$ETB\big|_{m=l+1} - ETB\big|_{m=l} = \frac{1}{n}\sum_{i=1}^{n}\left(\int_0^1 z\, g_{l+i}(z)dz - \int_0^1 z\, g_{l+i-1}(z)dz\right) = \frac{1}{n}\sum_{i=1}^{n}\left(\int_0^1 z\left(g_{l+i}(z) - g_{l+i-1}(z)\right)dz\right), \quad (37)$$

where $g_k(z)$ refers to (19).

According to Lemma 2(b), we have $\int_0^1 z(g_{l+i}(z)-g_{l+i-1}(z)$ <0. Therefore $ETB\big|_{m=l+1}-ETB\big|_{m=l}$ <0.

Theorem 3(a) has been proved.

For Theorem 3(b), we can prove it by showing $A(l+1)-A(l)$ >0 where $A(l)=ETB\big|_{m=l+1}-ETB\big|_{m=l}$.

$$A(l+1)-A(l)=\frac{1}{n}\sum_{i=1}^{n}\int_0^1 z(g_{l+i+1}(z)-g_{l+i}(z))-z(g_{l+i}(z)-g_{l+i-1}(z))dz$$

$$=\frac{1}{n}\sum_{i=1}^{n}\int_0^1 z(g_{l+i+1}(z)-2g_{l+i}(z)+g_{l+i-1}(z))dz$$

Denoting $G(z)=[g_{l+i+1}(z)-2g_{l+i}(z)+g_{l+i-1}(z)$, according to Equation (37), we have

$$G(z)=[(l+i+1)(1-F(z))^2-2(l+i)(1-F(z))+(l+i-1)]\cdot f(z)(1-F(z))^{l+i-2}$$

$$=[(1-F(z))-1][(l+i+1)(1-F(z))-(l+i-1)]\cdot f(z)(1-F(z))^{l+i-2}$$
$$=-F(z)[(l+i+1)(1-F(z))-(l+i-1)]\cdot f(z)F(z))^{l+i-2}.$$

Solving equation $(l+i+1)(1-F(z))-(l+i-1)$ =0, we get its critical point (denoted as a'):

$$a'=F^{-1}(2/(l+i+1))$$

We then have $G(z)\begin{cases}\le 0 & if \quad z\le a' \\ >0 & otherwise\end{cases}$.

$$A(l+1)-A(l)=-\frac{1}{n}\sum_{i=1}^{n}\int_0^{a'}\int_{g_{l+i+1}(z)-g_{l+i}(z)}^{g_{l+i}(z)-g_{l+i-1}(z)} zdydz+\frac{1}{n}\sum_{i=1}^{n}\int_{a'}^{1}\int_{g_{l+i}(z)-g_{l+i-1}(z)}^{g_{l+i+1}(z)-g_{l+i}(z)} zdydz$$

$$>-\frac{1}{n}\sum_{i=1}^{n}\int_0^{a'}\int_{g_{l+i+1}(z)-g_{l+i}(z)}^{g_{l+i}(z)-g_{l+i-1}(z)} a'dydz+\frac{1}{n}\sum_{i=1}^{n}\int_{a'}^{1}\int_{g_{l+i}(z)-g_{l+i-1}(z)}^{g_{l+i+1}(z)-g_{l+i}(z)} a'dydz$$

$$=\frac{a'}{n}\sum_{i=1}^{n}\int_0^{a'}-\int_{g_{l+i+1}(z)-g_{l+i}(z)}^{g_{l+i}(z)-g_{l+i-1}(z)} dydz+\frac{a'}{n}\sum_{i=1}^{n}\int_{a'}^{1}\int_{g_{l+i}(z)-g_{l+i-1}(z)}^{g_{l+i+1}(z)-g_{l+i}(z)} dydz$$

$$=\frac{a'}{n}\sum_{i=1}^{n}\int_0^{a'}G(z)dz+\frac{a'}{n}\sum_{i=1}^{n}\int_{a'}^{1}G(z)dz=\frac{a'}{n}\sum_{i=1}^{n}\int_0^{1}G(z)dz. \tag{38}$$

Because $g_{l+i}(z)$ is a PDF where $0\le z\le 1$, we have $\int_0^1 g_{l+i}(z)dz=1$, and then

$$\int_0^1 G(z)dz=\int_0^1[g_{l+i+1}(z)-g_{l+i}(z)]-[g_{l+i}(z)-g_{l+i-1}(z)]dz=0 \tag{39}$$

Substituting Equation (39) into Equation (38), we have $A(l+1)-A(l)>0$.

Therefore, Theorem 3(b) has been proved.

Appendix F. Proof of THEOREM 5

Similar to the proof of Theorem 3, we only need to prove that ETB (see Equation (21)) has the properties as mentioned in Theorem 5 as ESC is a constant.

We can prove the theorem by showing $ETB\big|_{m\leftarrow m+\vartriangle k} - ETB\big|_{n\leftarrow n+\vartriangle k}$ <0 where $\vartriangle k$ is any positive integer.

Using Equation (20), we have $ETB\big|_{m\leftarrow m+\vartriangle k} - ETB\big|_{n\leftarrow n+\vartriangle k} = \frac{1}{n}\sum_{i=1}^{n}\int_0^1 z\, g_{m+i+\vartriangle k}(z)dz - \frac{1}{n+\vartriangle k}\sum_{i=1}^{n+\vartriangle k}\int_0^1 z\, g_{m+i}(z)dz$

$$=\int_0^1 [\frac{1}{n}\sum_{k=m+\vartriangle k}^{n+m+\vartriangle k-1} z(kf(z)(1-F(z))^{k-1} - \frac{1}{n+\vartriangle k}\sum_{k=m}^{n+m+\vartriangle k-1} z(kf(z)(1-F(z))^{k-1}]dz$$
$$=\frac{1}{n}\sum_{k=m+\vartriangle k}^{n+m+\vartriangle k-1}\int_0^1 z(kf(z)(1-F(z))^{k-1}dz - \frac{1}{n+\vartriangle k}\sum_{k=m}^{n+m+\vartriangle k-1}\int_0^1 z(kf(z)(1-F(z))^{k-1}dz\,.$$

The first term $\frac{1}{n}\sum_{k=m+\vartriangle k}^{n+m+\vartriangle k-1}\int_0^1 z(kf(z)(1-F(z))^{k-1}dz$, is the average value of the sum of

$\int_0^1 z(kf(z)(1-F(z))^{k-1}dz$ with $k=m+\vartriangle k,\ldots,\ m+\vartriangle k+n-1$.

The second term $\frac{1}{n+\vartriangle k}\sum_{k=m}^{n+m+\vartriangle k-1}\int_0^1 z(kf(z)(1-F(z))^{k-1}dz$, is the average value of $\int_0^1 z(kf(z)(1-F(z))^{k-1}dz$ with $k=m,\ldots,m+n+\vartriangle k$ -1 which has $\vartriangle k$ extra addends compared with the first term.

All *n* addends in the first term are included in the second term, and $\vartriangle k$ extra addends in the second term are $\int_0^1 z(kf(z)(1-F(z))^{k-1}dz$ with $k=m,\ldots,m+\vartriangle k$ -1.

According to Lemma 2(b), $\int_0^1 z(k_2 f(z)(1-F(z))^{k_2-1}dz < \int_0^1 z(k_1 f(z)(1-F(z))^{k_1-1}dz$ for every $k_2 \ge k_1$.

The minimum of the $\vartriangle k$ extra addends then is $\int_0^1 z(kf(z)(1-F(z))^{k-1}dz$ at k= $m+\vartriangle k$ -1, which is larger than the maximum one in the other *n* addends ($\int_0^1 z(kf(z)(1-F(z))^{k-1}dz$ at k= $m+\vartriangle k$).

We therefore have $\frac{1}{\vartriangle k}\sum_{k=m_e}^{m_e+\vartriangle k-1}\int_0^1 z(kf(z)(1-F(z))^{k-1}dz > \frac{1}{n}\sum_{k=m_e+\vartriangle k}^{n+m_e+\vartriangle k-1}\int_0^1 z(kf(z)(1-F(z))^{k-1}dz$, and

$ETB\big|_{m\leftarrow m+1}) - ETB\big|_{n\leftarrow n+1})$ <0. Theorem 5 has been proved.

Appendix G. Proof of THEOREM 6

We denote the change of EDC^* as ΔEDC^* with the increase in *n* from *l* to *l*+1. If we can demonstrate ΔEDC^* <0, the proof is done.

With the increase in *n*, the optimal solution (x_e^*, y_e^*, m_e^*) and then EDC^* of Model M change subsequently. ΔEDC^* can be decomposed into two parts by two procedures, respectively. First we let *n* increase from *l* to *l*+1 and keep (x_e^*, y_e^*, m_e^*) constant to obtain the first part of the change of EDC^* , ΔEDC_1 . Next we let (x_e^*, y_e^*, m_e^*) respond to the first change to obtain the other change of EDC^* , ΔEDC_2 .

$\Delta EDC^* = \Delta EDC_1 + \Delta EDC_2$.

For the first procedure, according to Theorem 4, we can obtain a reduction ΔEDC_1 <0.

For the second procedure, if (x_e^*, y_e^*, m_e^*) changes, if the solution can be improved, we then obtain the other reduction ΔEDC_2 <0. Otherwise, (x_e^*, y_e^*, m_e^*) does not change and we have ΔEDC_2 =0.

In result, we obtain the total reduction in EDC^* , $\Delta EDC^* < 0$. Therefore, Theorem 6 has been proved.

Appendix H. THEOREM 7

THEOREM 7. If there are two different m_e either for the ESA policy or NN, with an increase in *n* the marginal effect of *n* at the smaller m_e on reducing EDC is bigger than that of *n* at the other larger m_e .

The proof is similar to that of Theorem 3, and is omitted here.

Publications in the Report Series Research[*] in Management

ERIM Research Program: "Business Processes, Logistics and Information Systems"

2009

How to Normalize Co-Occurrence Data? An Analysis of Some Well-Known Similarity Measures
Nees Jan van Eck and Ludo Waltman
ERS-2009-001-LIS
http://hdl.handle.net/1765/14528

Spare Parts Logistics and Installed Base Information
Muhammad N. Jalil, Rob A. Zuidwijk, Moritz Fleischmann, and Jo A.E.E. van Nunen
ERS-2009-002-LIS
http://hdl.handle.net/1765/14529

Open Location Management in Automated Warehousing Systems
Yugang YU and René B.M. de Koster
ERS-2009-004-LIS
http://hdl.handle.net/1765/14615

---

[*] A complete overview of the ERIM Report Series Research in Management:
https://ep.eur.nl/handle/1765/1

ERIM Research Programs:
LIS Business Processes, Logistics and Information Systems
ORG Organizing for Performance
MKT Marketing
F&A Finance and Accounting
STR Strategy and Entrepreneurship